THE FACE OF MARS

Mariner 9

National Aeronautics and Space Administration

Jet Propulsion Laboratory/California Institute of Technology

Pasadena, California
June 1972

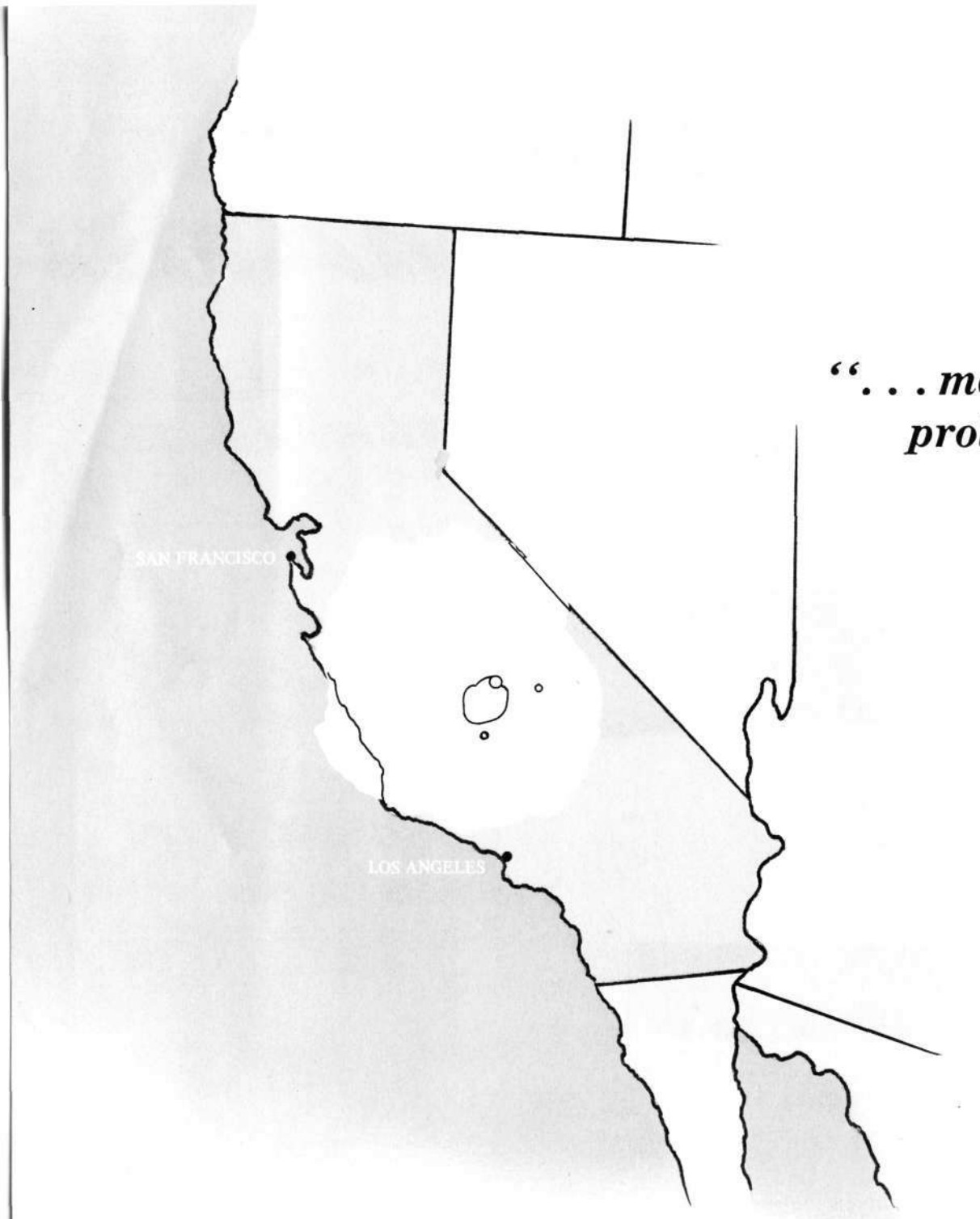

Sketch showing the comparison in size of the Martian volcanic mountain, Nix Olympica, with California.

". . . man's past in space is but a prologue in his insatiable search for knowledge of his environment."

W. H. Pickering

Pasadena Star News, January 1, 1972

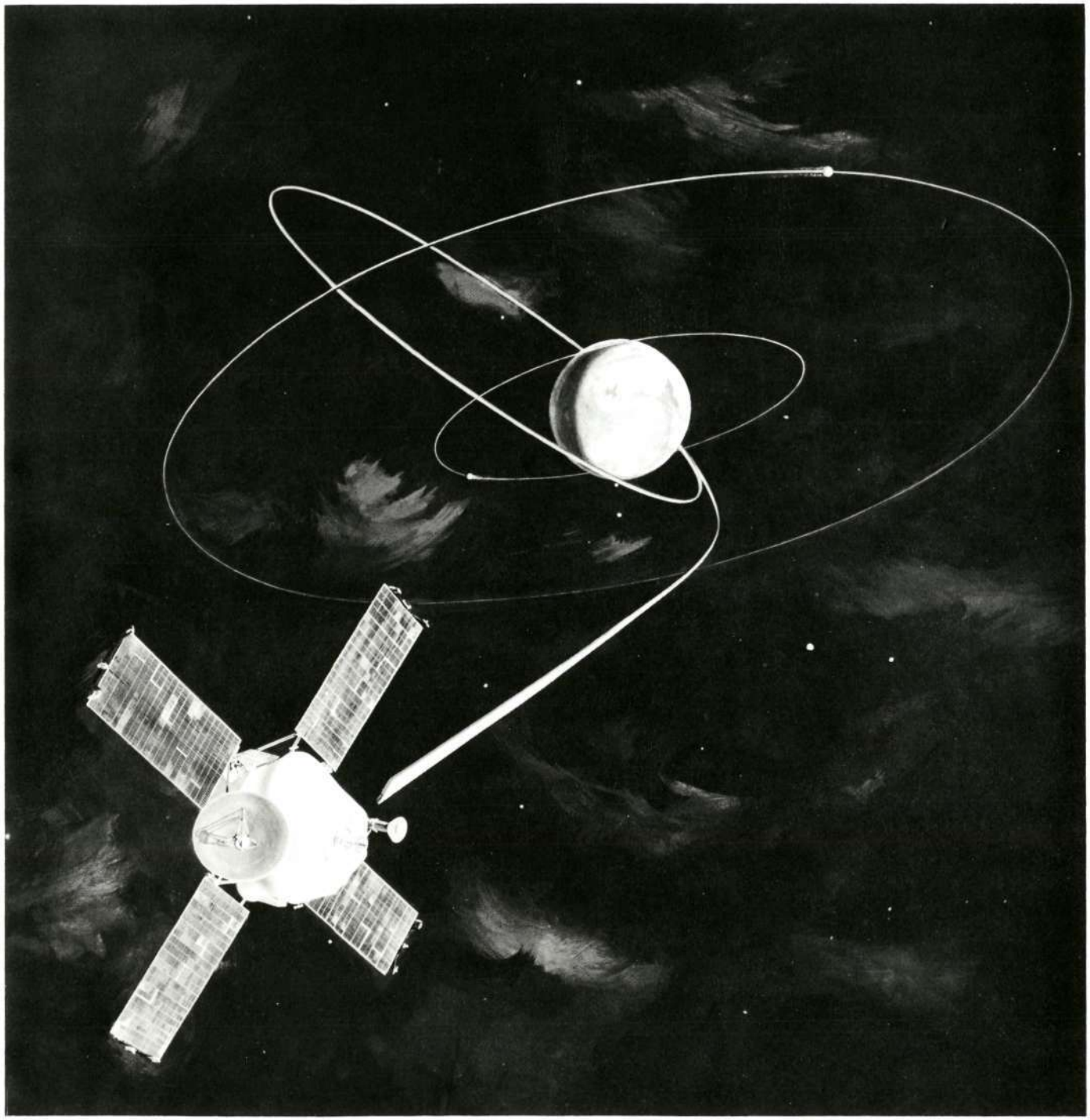

Introduction

This document provides a brief summary of salient science results obtained from the Mariner 9 mission through early June 1972. Mariner 9, the fourth U.S.A. spacecraft to make the journey to Mars and the first to orbit the planet, represents the latest in the evolving family of Mariner spacecraft.

The previous missions to Mars, made in 1965 and 1969 by Mariners 4, 6, and 7, were flyby missions and provided only a brief glimpse of the planet. Although their views of Mars were more limited, the missions were invaluable because they supplied man with the first close look at Mars and formed the basis for the Mariner 9 technology. In turn, the data from Mariner 9 will provide information and technological experience from which the Viking 1975 Project will benefit. Therefore, the success of Mariner 9 will also be reflected in the Viking orbiter spacecraft, which will transport the Viking instrumented capsules to Mars for their landing on the planet's surface in 1976.

Mission Event Summary

Mariner 9 was launched from Cape Kennedy, Florida, on May 30, 1971. On June 5, a trajectory correction was made so accurately that no other midcourse corrections were necessary for the entire 167-day flight to Mars.

On November 14, the spacecraft was inserted successfully into orbit by a 15-minute motor burn. Two days after insertion, on the fourth revolution around Mars, the spacecraft's orbit was corrected by a 6-second firing of the rocket engines. However, because of a previously unknown gravity-field variation in the planet's equatorial plane, the average orbital period (11.97 hours) was found to be slightly too short, gradually changing the time relationship of the low point in the orbit (periapsis) to the tracking stations, which would eventually affect data playbacks.

At the time of Mariner's arrival, the planet-wide dust storm, which had been detected from Earth starting in late September, was still obscuring the surface features of Mars. Although this dust storm was a bonus to scientists and ultimately enabled many additional findings, it was a major factor in the decision to change the mission plan, since no systematic surface picture coverage could be established to enable the start of mapping or dynamic variation objectives.

A second trim maneuver was made on December 30, 47 days after insertion. This maneuver corrected the orbital period, coordinating the periapsis-passage timing with the view period of the 64-meter (210-foot) antenna at the Goldstone tracking station in California. The maneuver also changed the periapsis altitude from 1387 to 1650 kilometers (862 to 1025 miles), allowing broader television coverage and permitting the mapping objective to be fulfilled. This second trim was the last maneuver performed. Mariner will remain in that orbit for the rest of its operational life.

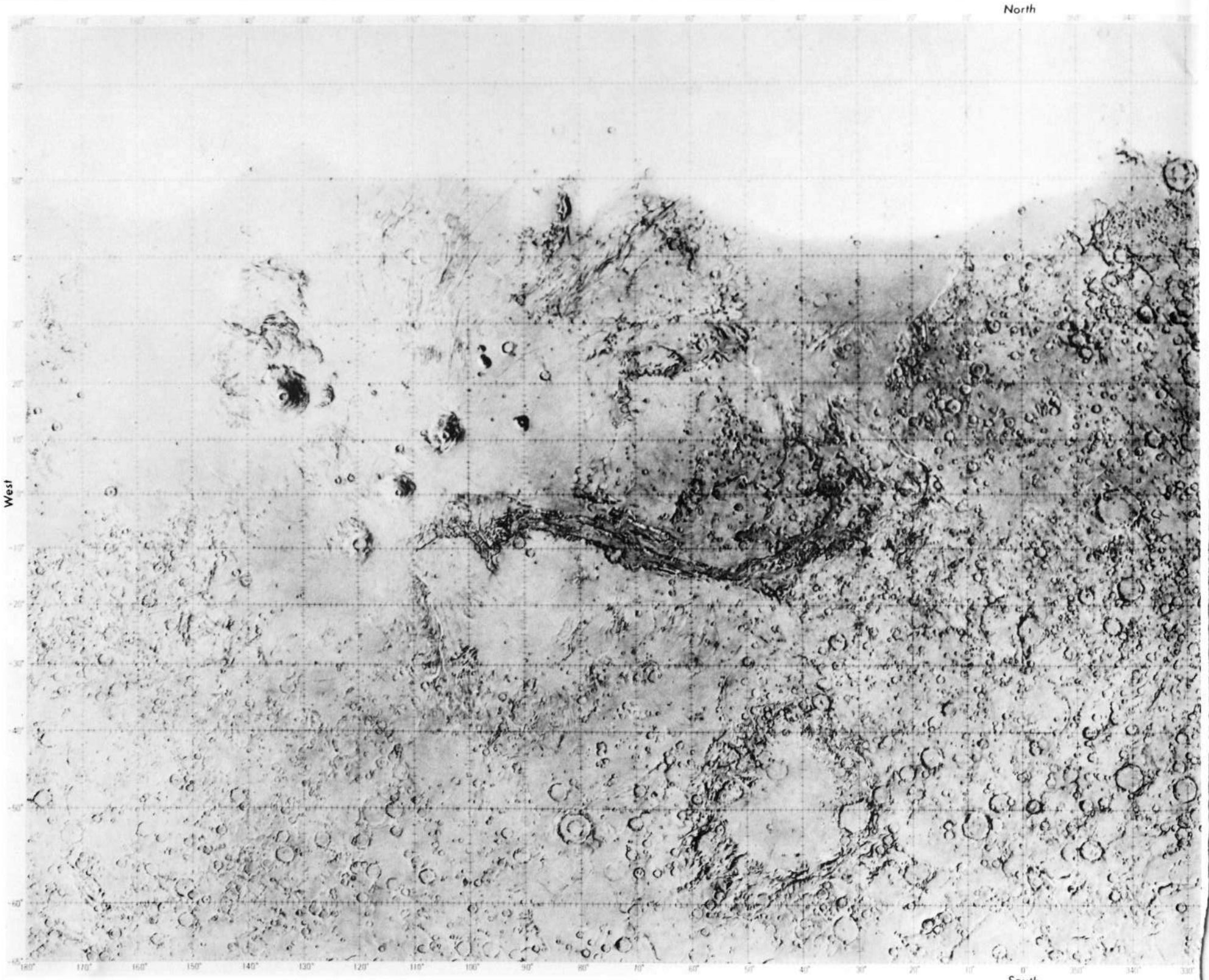
North
West
South

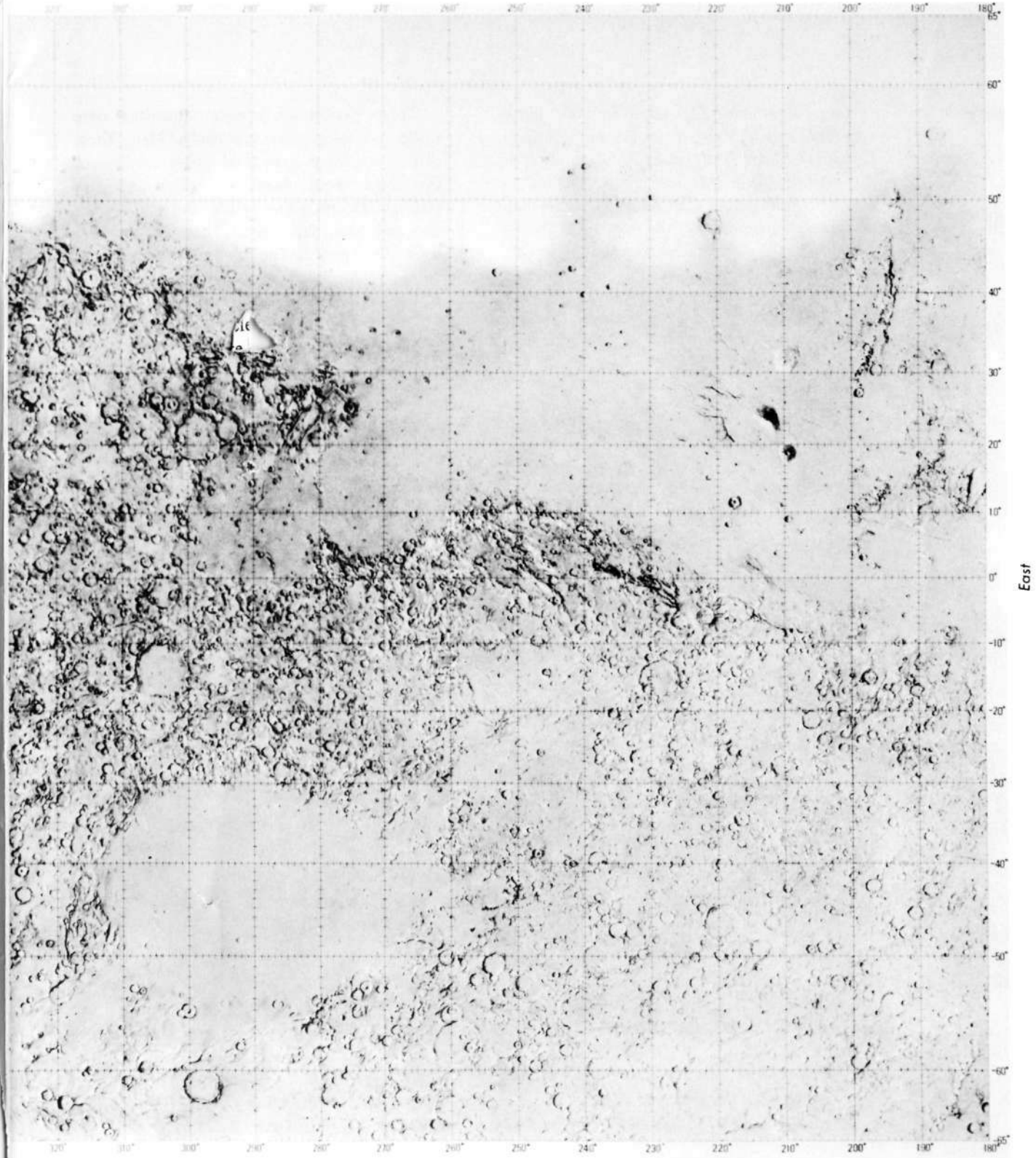

Preliminary airbrushed rendition of a Mercator projection map produced by the U.S. Geological Survey using Mariner 9 television pictures. The map shows the topography of Mars from 65° south to 65° north latitude. The region north of 40° latitude was cloud covered at the time the pictures were taken.

The southern hemisphere, exclusive of the polar region, is Moonlike, exhibiting many impact craters and two large mare-basin type features. The western half of the northern hemisphere shows few impact craters. It is assumed that the original impact features have been destroyed through the formation of geologic structures similar to those found on Earth (for example, the large shield volcano mounds and large canyon). To a lesser extent, this is also the case in the eastern part of the northern hemisphere. Specific features of areas located on this map are discussed in this booklet of Mariner 9 science results.

Science Findings

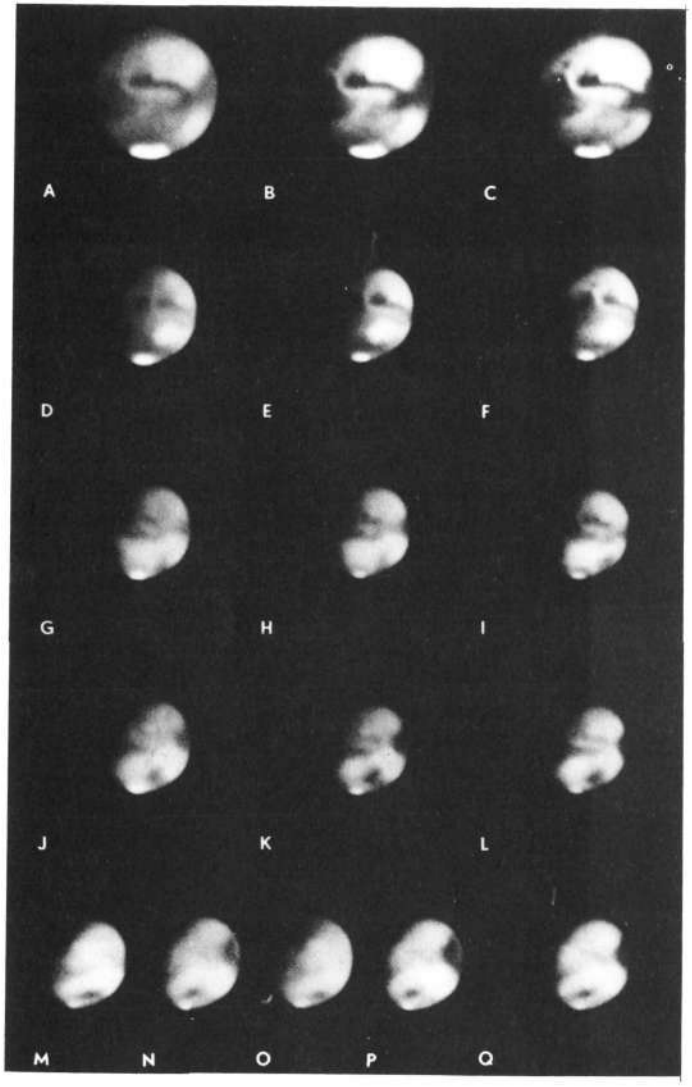

Figure 1. Picture sequence, taken by Earth-based telescope, showing the region of the dust storm before (A-C) and after (D-Q) its outbreak. The pictures were taken using infrared, red, and green filters. (Photographs are by courtesy of New Mexico State University.)

On September 22, observers on Earth recorded a yellow cloud in the mid-southern latitudes of Mars. The cloud spread rapidly over the rest of the planet (see Figure 1), and in about 2 weeks even the south polar cap had disappeared from view of the telescopes. By the fifth week, the dust storm had reached its peak, far exceeding all previously observed storms in intensity. Figure 2 shows the planet as it looked on October 20, 21, and 22, about 3 weeks before insertion of Mariner 9 into orbit around Mars.

Three pre-orbital science sequences were taken as the spacecraft approached Mars. These picture sequences gave total global coverage of the dust-covered planet, on which only five distinct features were visible: the south polar cap and four dark spots. These features are shown in Figure 3. The small south polar cap is visible at the bottom of the planet's disk in Figure 3a. Some high-resolution pictures (taken by the narrow-angle television camera) of the south polar cap are shown in Figure 4. Although the surface detail could not be seen

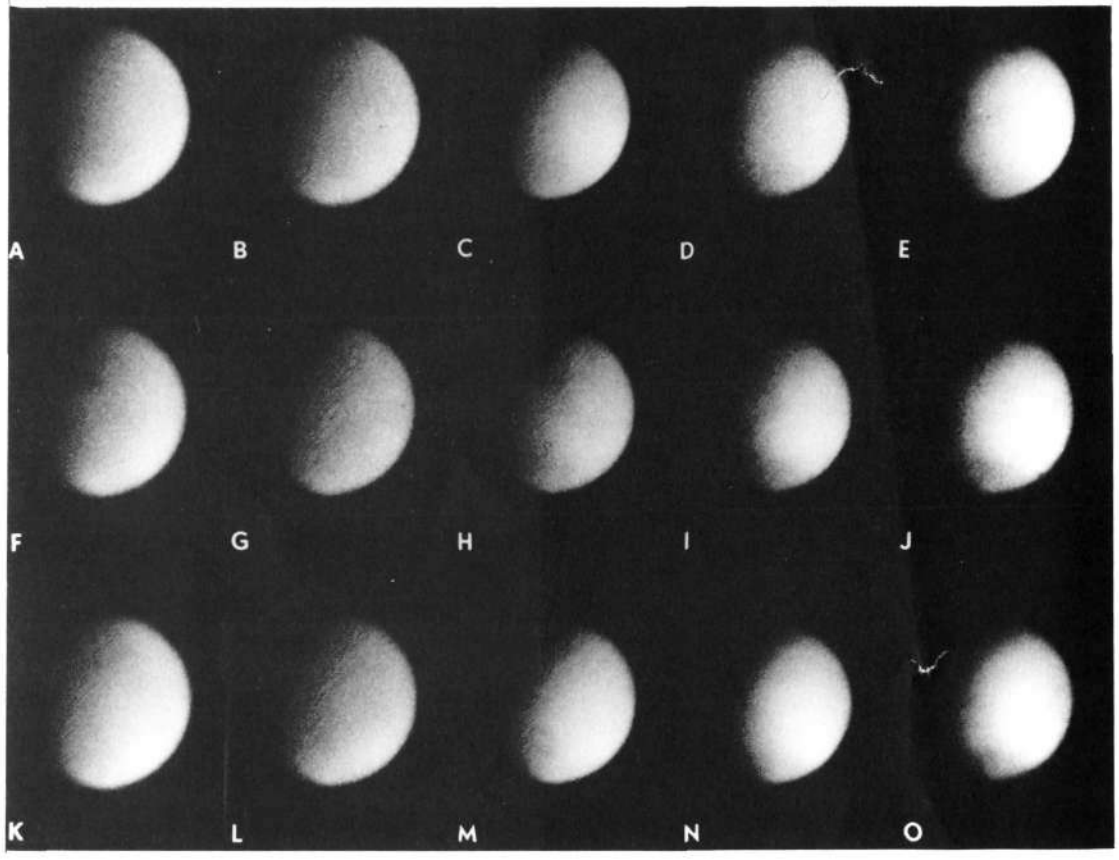

Figure 2. Picture sequence, taken by Earth-based telescope, showing the dust storm as it looked on October 20, 21, and 22. The pictures were taken using infrared, red, green, blue, and violet filters. (Photographs are by courtesy of New Mexico State University.)

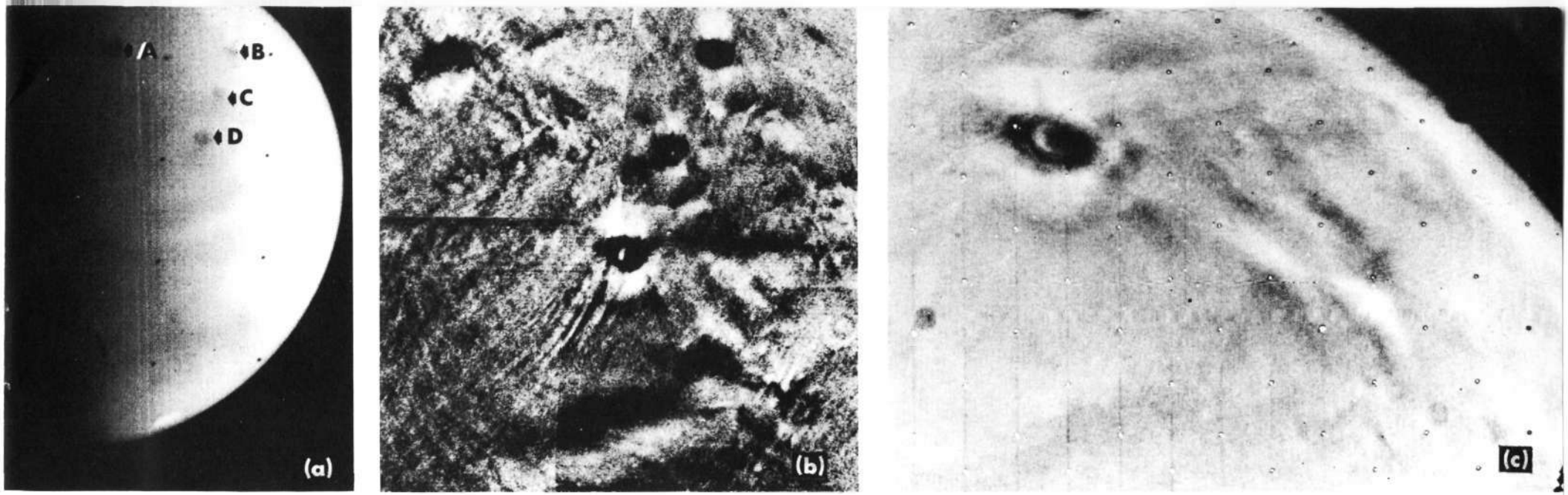

Figure 3. (a) Pre-orbital science picture showing the four dark spots: Nix Olympica (A), North (B), Middle (C), and South (D). (b) Computer-processed mosaic of the four spots showing atmospheric streaks running 1000 kilometers (620 miles) south of South Spot. (c) Computer-processed picture of South Spot taken on November 25.

Figure 4. Details of the south polar cap. Various patterns in the subliming frost cap are recorded in the five small frames. Their locations are marked in the large picture.

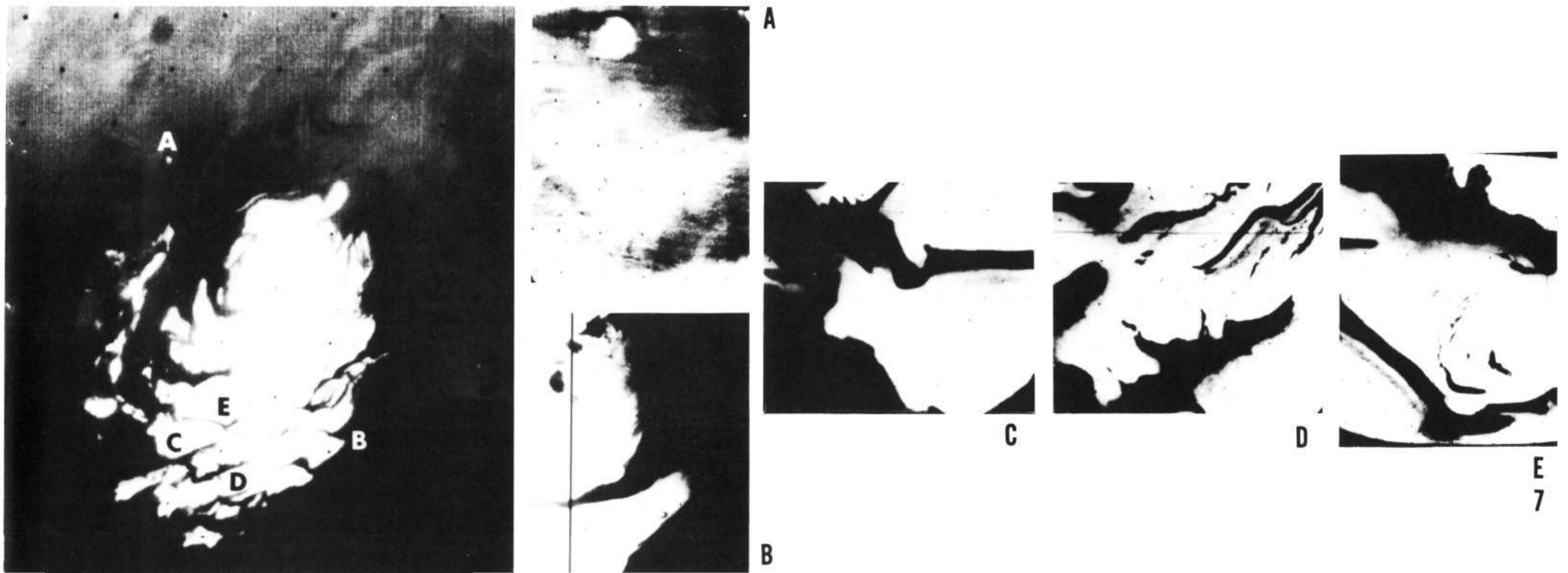

because of the atmospheric dust, the residual cap area appeared smooth. In contrast to the 1969 Mariner 7 pictures, Mariner 9 showed the dark markings between the parts of the white residual cap as light features (see Figure 5). One of the four dark spots was subsequently identified as Nix Olympica (Snows of Olympus). In early Mariner 9 orbital pictures, this region showed a dark mountain standing above the Martian dust storm. The other three spots were provisionally labeled North, Middle, and South Spots. All four spots are shown in Figure 6.

Nix Olympica and North Spot each contain intersecting craters whose floors lie at different elevations. The craters are rimless or very low rimmed; sharp edges are strikingly absent. All four dark spots have been determined to be volcanic in origin, but South Spot, which is about 125 kilometers (75 miles) across, is the largest volcanic caldera ever observed.

After orbit insertion, the south polar cap became a prime target because it could be viewed by the ultraviolet spectrometer, infrared interferometer spectrometer, and the infrared radiometer. Three high-resolution pictures of the south polar cap, taken by Mariner 9 on November 19, 28, and December 1, are shown in Figure 7. The same local area is viewed in each case, and is indicated by a dark arrow on the accompanying low-resolution view (taken by the wide-angle television camera). The location of the south pole of Mars and the direction of the prime meridian are shown in white. In the high-resolution pictures, the maximum dimension corresponds to about 100 kilometers (62 miles) on the Martian surface. The low-resolution view is presented at ten times greater

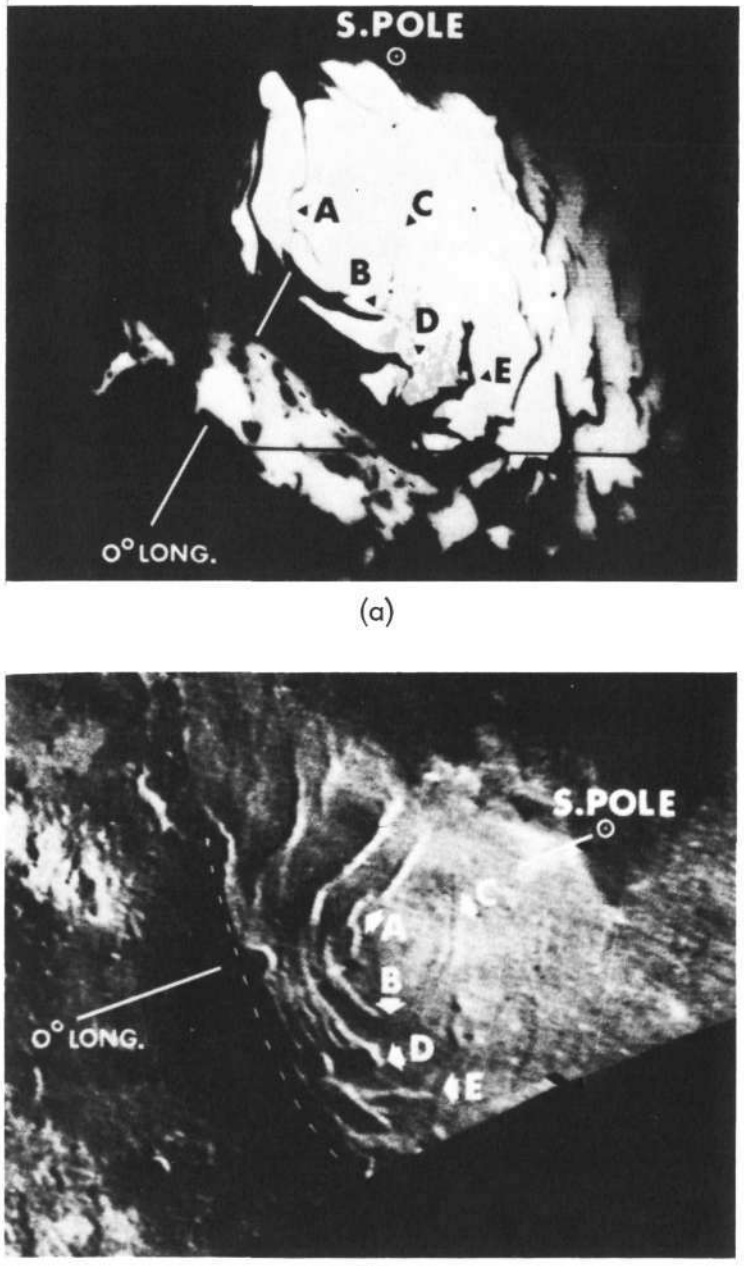

Figure 5. (a) Mariner 9 and (b) Mariner 7 views of the south polar cap showing correlation of dark markings in the Mariner 9 view of the cap with light markings in the Mariner 7 view.

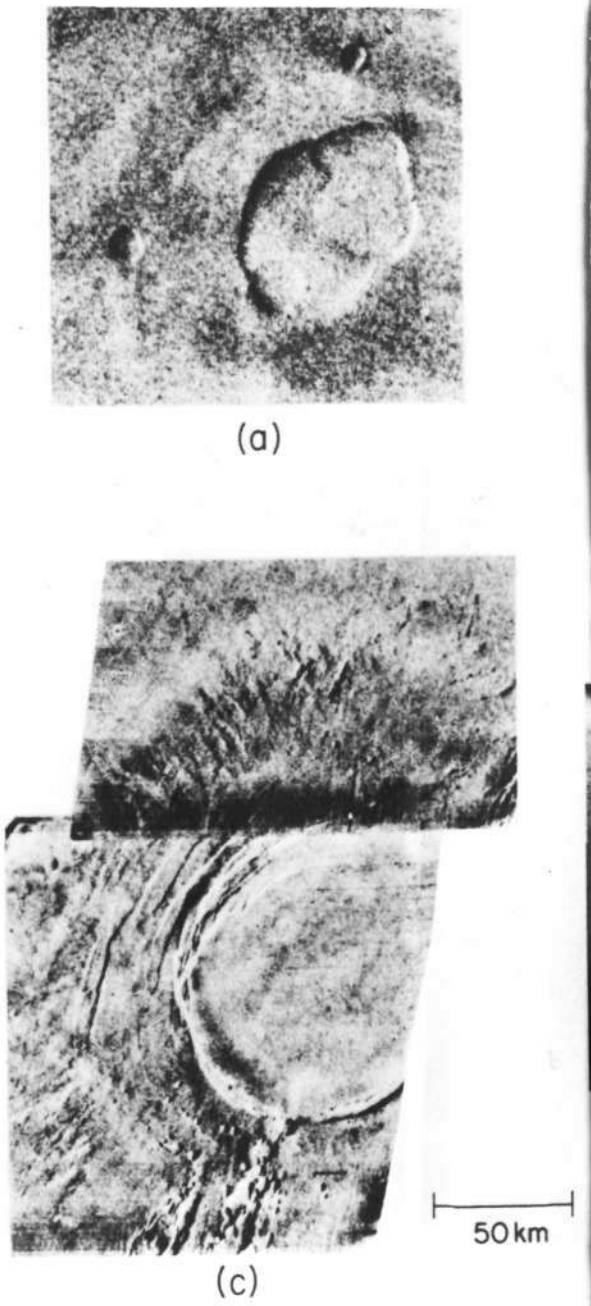

Figure 6. (a) Crater complex of Nix Olympica (c) South Spot crater. (d) Middle Spot.

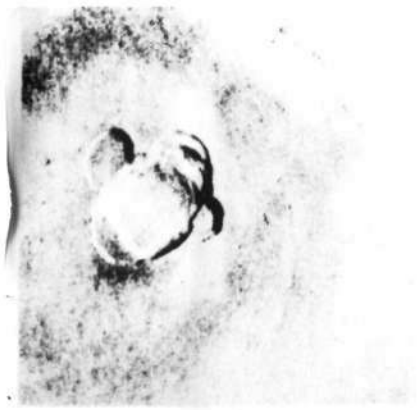

(b)

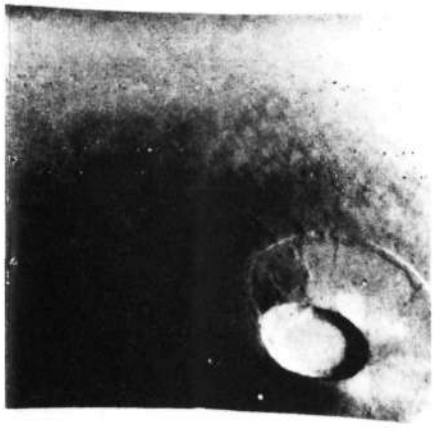

(d)

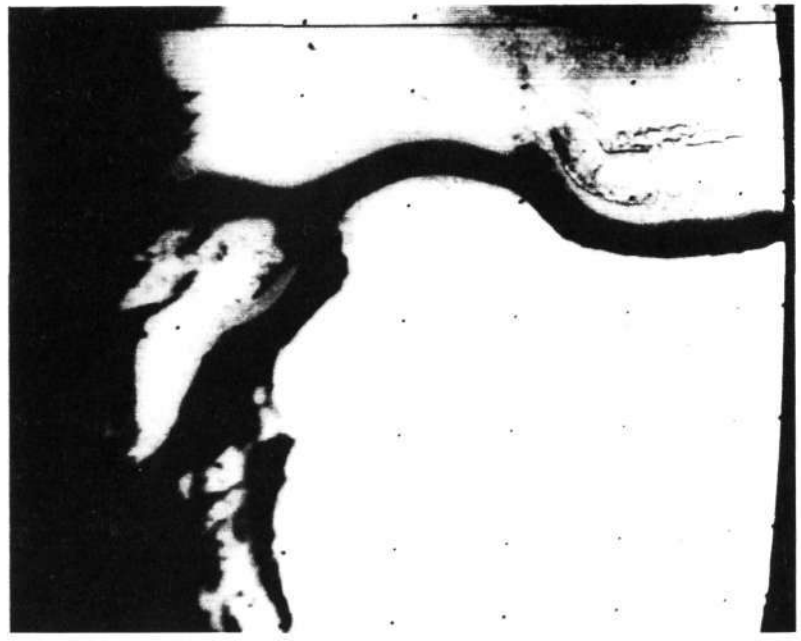

(b) Crater complex of North Spot.

Figure 7. Views of the south polar cap.

scale. Mariner 9 pictures displaying the gradual disappearance of the residual polar cap are shown in Figure 8. The south pole is located just off the residual cap area (about the center of the cap and just above the cap in the November 18 picture). Investigations have shown that the areas are smooth, and the lines are terraces, or changes in elevation, between the smooth, terraced terrain. The entire cap in the November 18 pictures covers about a 10° arc on the Martian surface. (This was reduced to about an 8° arc by December 24.)

Mariner 9 obtained the first close-up views of the Martian satellites, Phobos and Deimos. Both satellites are heavily cratered, indicating a probable age of several billion years. They are two of the darkest objects in our solar system ever to be photographed. Phobos has an albedo (reflective power) of about 5 percent, and Deimos about 6 percent.

Phobos the closer satellite, is about 25 kilometers (16 miles) long and about 21 kilometers (12 miles) wide. An especially striking feature is the 5.3-kilometer (3.3-mile) crater near the bottom (south pole) in Figure 9a and near the center in Figure 9b. The impact that produced the crater is close to the largest impact Phobos could have sustained without fracture and disruption. Many of the irregular edges on Phobos may have been produced by the breaking off of pieces on impact. Deimos, the farther satellite, is about 13-1/2 kilometers (8-1/2 miles) long and about 12 kilometers (7-1/2 miles) wide. Two clear crater-like depressions, each about 1-1/2 kilometers (1 mile) across, are apparent in Figure 10 near the terminator (region of shading that separates the day from the night side of the satellite). The deep cleft at the bottom is probably a valley about 1½ kilometers deep.

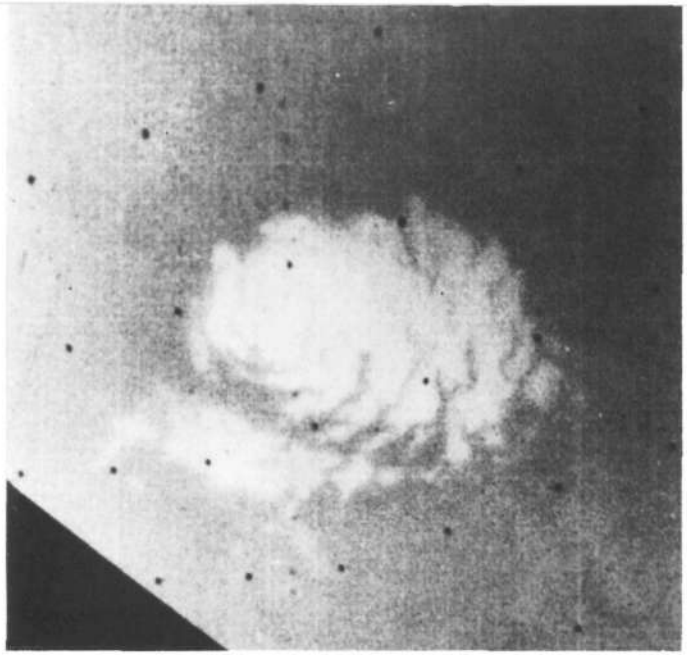

NOVEMBER 18

NOVEMBER 28

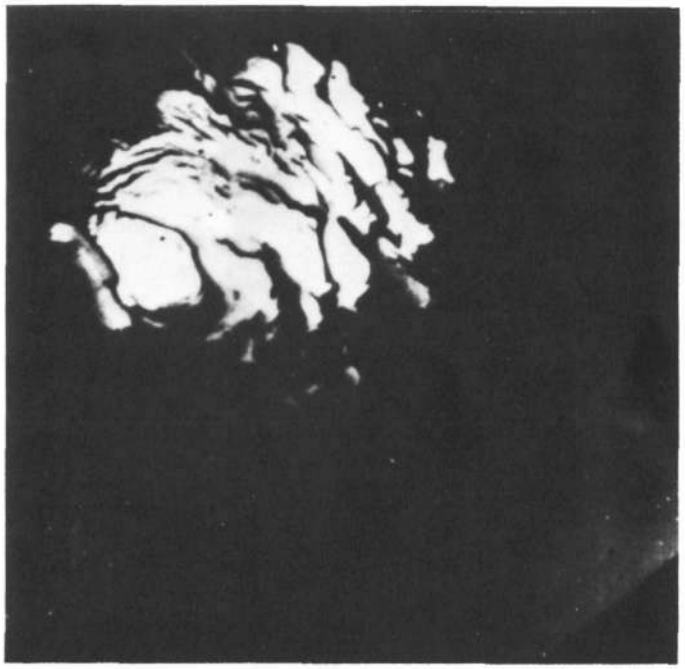

DECEMBER 13

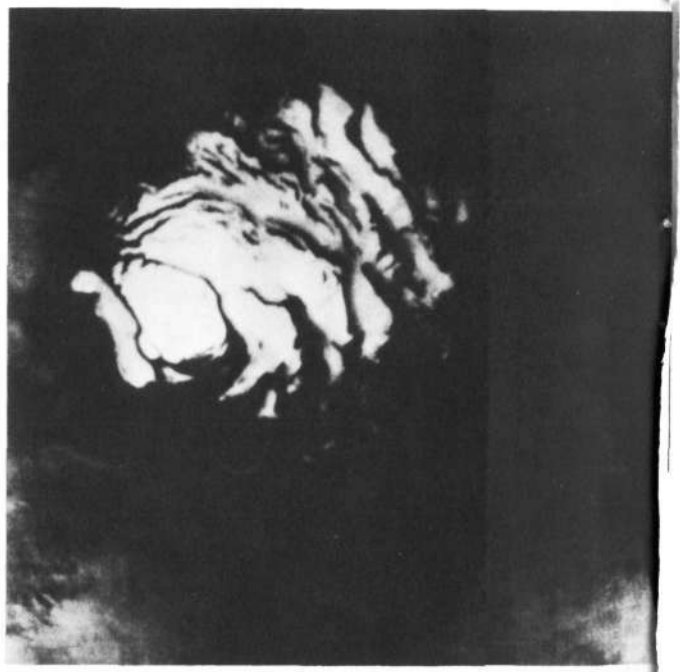

DECEMBER 24

Figure 8. Four early views of the south polar cap taken over a 36-day period.

Figure 9. Computer-processed pictures of Phobos. (a) View obtained at a distance of 14,440 kilometers (8973 miles). (b) View obtained at a distance of 5550 kilometers (3449 miles).

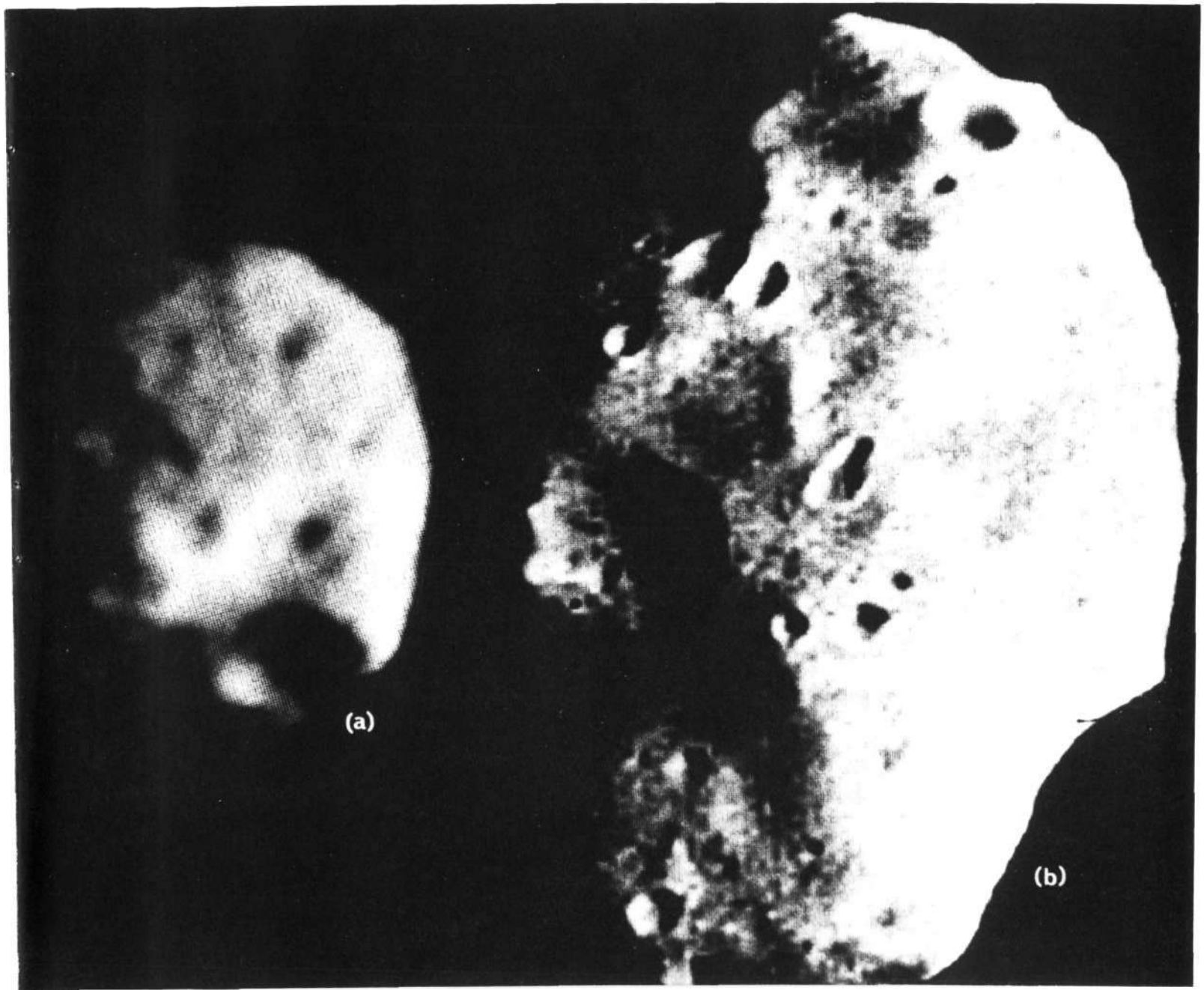

Figure 10. Computer-processed picture of Deimos obtained at a distance of 8830 kilometers (5487 miles).

In spite of the dust-laden Martian atmosphere, the nonvisual experiments also obtained data. The ultraviolet spectrometer recorded measurements of the upper atmosphere and found them comparable to those taken in 1969 by Mariners 6 and 7 (see Figures 11 and 12). Because Mariner 6 and 7 data showed that the most probable source of excitation of the carbon monoxide a-X and A-X bands was the solar electron and photon impact-induced dissociative excitation of carbon dioxide, the intensity of these bands as a function of altitude was used to determine the density distribution of carbon dioxide in the upper atmosphere. The scale height (vertical distribution) of these emissions was used to determine the temperature of the upper atmosphere. The emission rate of these two band systems as a function of altitude is shown in Figure 13 for a limb observation made on December 1, and is typical of the limb measurements made during the first 30 days.

In contrast to the spectra obtained by Mariners 6 and 7, the spectral shape of the Mariner 9 reflectance depended on what location on the planet was being observed. The overall spectral shape was determined by the relative amount of molecular or large particles scattering. Two examples of early Mars spectra are shown in Figures 14 and 15, together with the reflectance as a function of wavelength. [Reflectance is defined here as one-fourth the ratio of the intensity (photon cm^{-2} sec^{-1} $Å^{-1}$) of the region of Mars being observed to the solar flux (photon cm^{-2} sec^{-1} $Å^{-1}$).]

The dust storm changed the characteristics of ultraviolet reflectance from those in 1969, resulting in a reflectance of smaller magnitude. The dust, which dominated the ultraviolet light scattered from the disk of Mars, was a strong absorber in the ultraviolet.

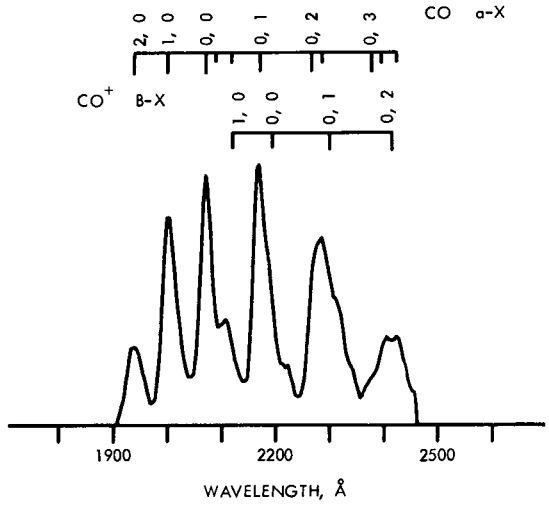

Figure 11. Airglow spectrum of Mars between 1910 and 2460 angstroms. (Ten angstroms equal 1 nanometer.) This calibrated spectrum was obtained by summing 20 individual spectral observations, as was the spectrum in Figure 12.

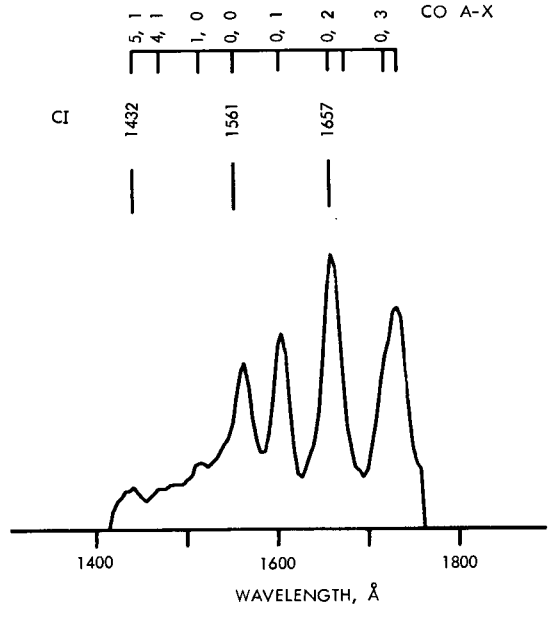

Figure 12. Airglow spectrum of Mars between 1420 and 1760 angstroms.

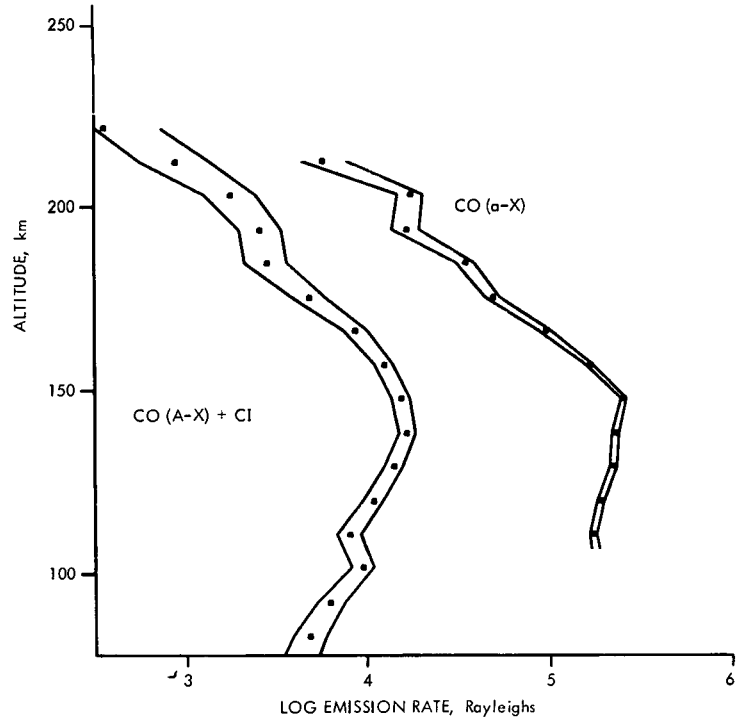

Figure 13. Emission rates of the carbon monoxide a-X Cameron bands and the sum of the carbon monoxide A-X fourth positive bands and the atomic carbon lines as a function of altitude. Data points are dots; envelopes represent a ±2 standard deviation error derived from counting statistics.

The most significant findings by the infrared interferometer spectrometer during the early part of the mission were related to the atmospheric dust: its chemical composition and its effect upon the thermal balance of the planet and its atmosphere. The locations and shapes of the silicate features (reststrahlen) appearing in the spectra (see Figure 16) are similar to those of terrestrial rocks and minerals which contain intermediate amounts (55 to 65 percent) of silicon oxide. This indicates that Mars has undergone planetary differentiation . . . a process of great geologic and exobiologic significance. The reststrahlen intensity indicates a substantial opaqueness for the dust, especially in the regions away from the south polar cap and high plateaus.

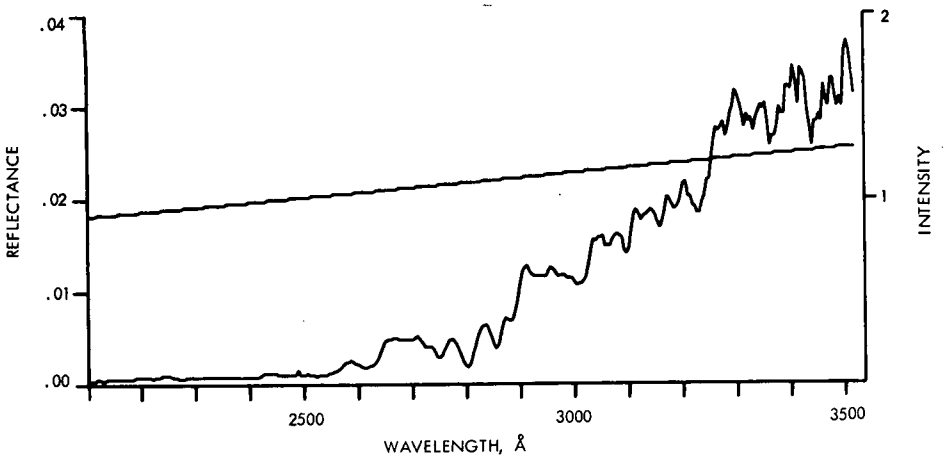

Figure 14. Ultraviolet reflectance in dusty region. The intensity of the ultraviolet spectrum was observed on Mars near 45° south latitude. [Units on the right-hand vertical scale are 10^{13} photons cm^{-2} sec^{-1} (14 Å)$^{-1}$.]

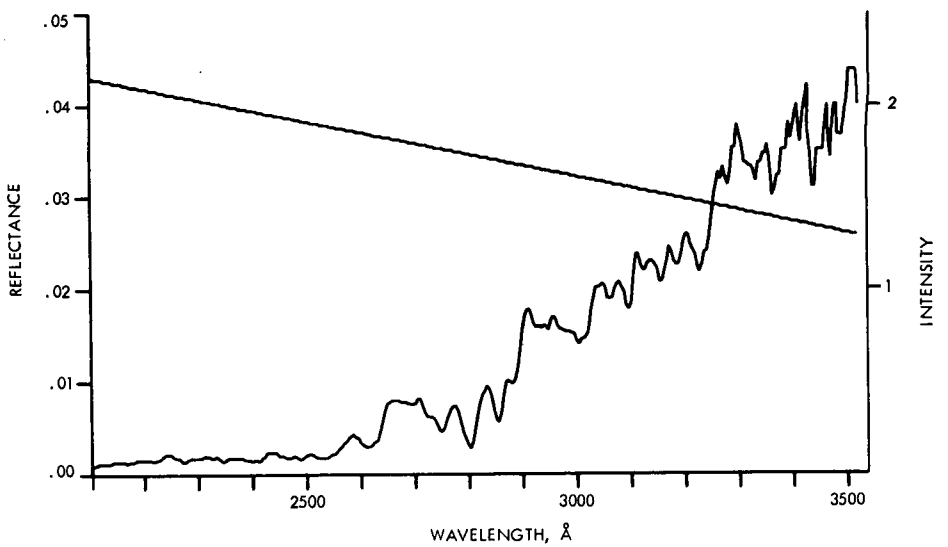

Figure 15. Ultraviolet reflectance in polar region. The intensity and reflectance of Mars were obtained near 86° south latitude. [Units on the right-hand vertical scale are 10^{13} photons cm^{-2} sec^{-1} (14 Å)$^{-1}$.]

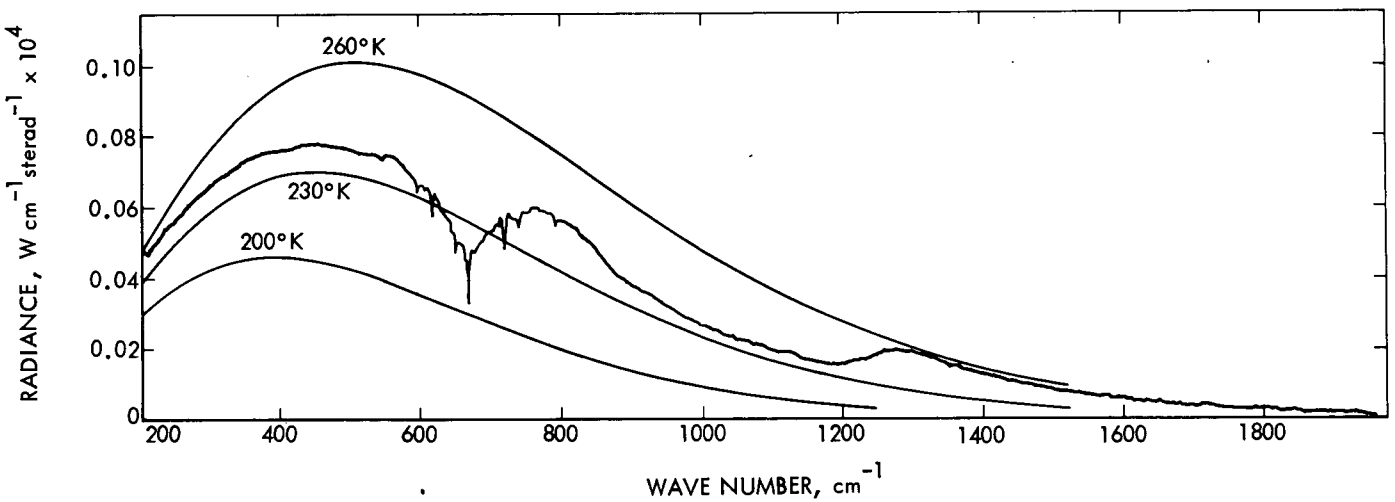

Figure 16. Example of non-polar thermal infrared emission spectrum, which is the average of six spectra obtained on November 17, 1971. Three blackbody curves are included for comparison. ("Wave number, cm^{-1}" is the number of full waves per centimeter.)

Under normal, clear atmospheric conditions, it was expected that mid-afternoon surface temperatures would be higher than atmospheric temperatures near the surface and that the atmospheric lapse rate (the rate at which the temperature drops with altitude) would be approximately 4°K/kilometer (2.2°F/1000 feet). During the dust storm, the surface actually was cooler than expected, and the atmosphere was almost isothermal (constant temperature with altitude). This occurred because the dust in the atmosphere absorbed and scattered much of the incident solar energy. Thus, the atmosphere received more thermal energy than normal, and the surface received less.

Polar spectra obtained by the infrared interferometer spectrometer showed rotational lines of water vapor in the region between 200 and 350 cm^{-1}. Water vapor spectral features appeared more weakly over other regions of the planet.

The infrared radiometer obtained surface temperature data that were in substantial agreement with data from the infrared interferometer spectrometer. Because of the narrower field of view of the radiometer, however, the structure associated with some of the small temperature variations could be seen. These variations were caused primarily by the cap and the higher-altitude areas.

Based on 1969 data, the surface temperatures at latitudes of between -20° and -30° south were expected to range from about 175°K (-145°F) near the morning terminator to 280°K (+44°F) near local noon. The actual observed brightness temperatures at those latitudes early in the mission when the atmosphere was dusty were about 205°K (-91°F) just before sunrise to about 255°K (-1°F) reached at about 3:00 p.m. Mars time (see Figure 17). As the dust cleared, however, the infrared radiometer observed that temperatures were closer to those predicted, as shown by the jagged lines in that figure. The residual polar cap appeared 35°K (63°F) colder than the surrounding terrain.

Atmospheric temperature profiles obtained from S-band occultation entry data for the first nine revolutions around Mars are shown in Figure 18. Profiles for exit data are shown in Figure 19. Most early Mariner 9 temperature profiles showed an isothermal regime near the surface, once again attributed to the planet-wide dust storm in progress.

Occultation data showed that the density and temperature of the Martian ionosphere have been reduced since 1969. The most notable difference between measurements from Mariner 9 and earlier spacecraft was the increased altitude of the ionization peak, which showed that the atmospheric regions below 145 kilometers (90 miles) were warmer than before.

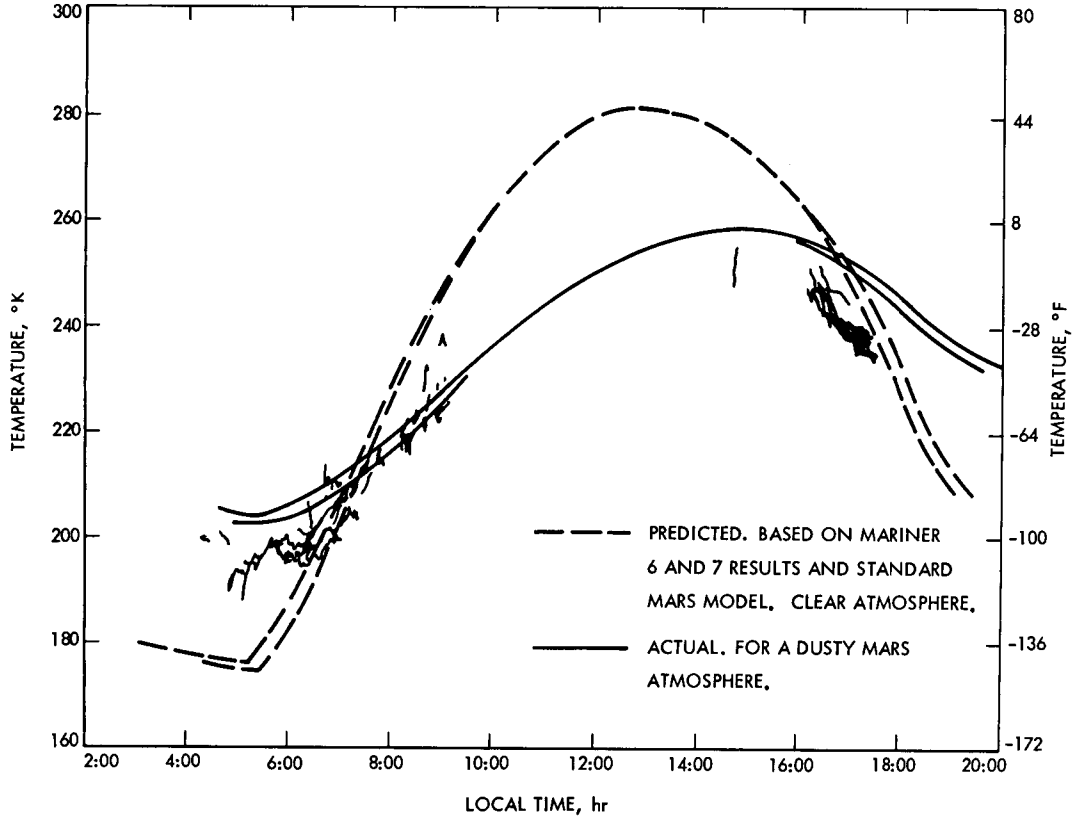

Figure 17. Temperatures of the Martian surface versus local time. Note that the surface temperature excursions are considerably less severe with the heavily dust-laden atmosphere.

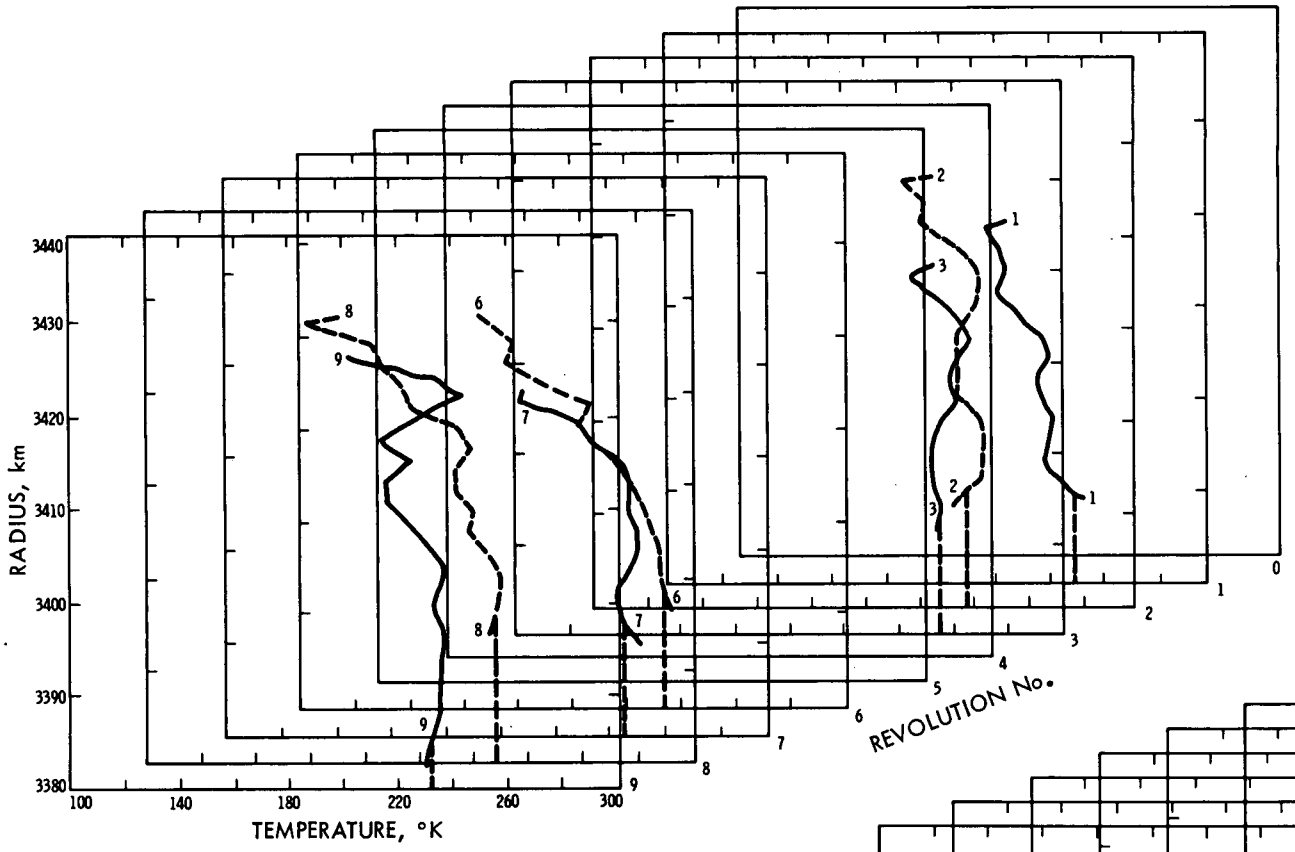

Figure 18. Atmospheric temperature profiles obtained from S-band entry occultation data for the first nine revolutions.

Figure 19. Atmospheric temperature profiles obtained from S-band exit occultation data for the first nine revolutions.

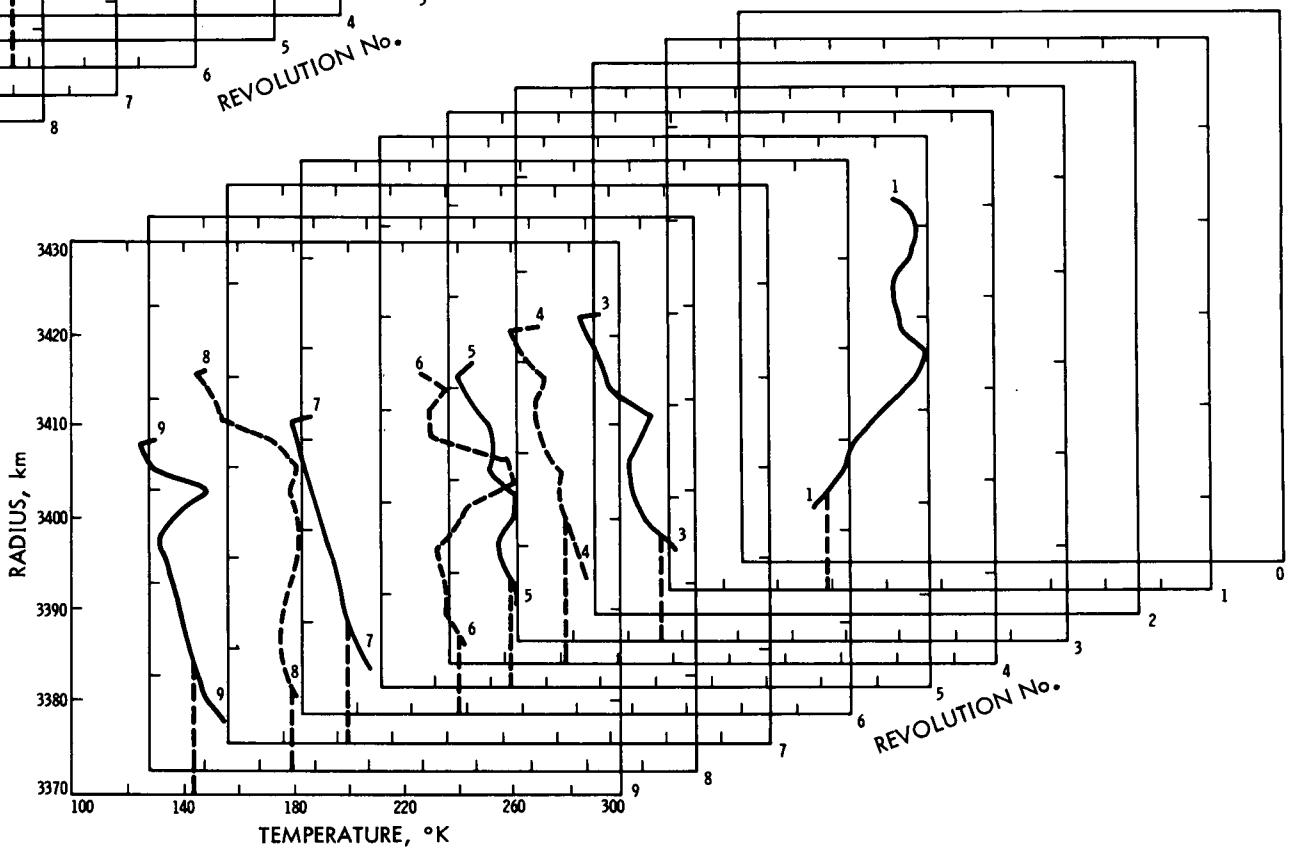

Variations in the gravity field on the surface of Mars were determined by means of the celestial mechanics experiment. The variations became apparent when the spacecraft orbit began to precess in an unexpected manner. The period variation underwent a complete cycle every 38 orbital revolutions (see Figure 20).

During the last half of December, indications began to appear that the dust storm was decreasing in intensity. Having achieved the desired orbital period and periapsis altitude 3 days earlier with the second trim, Mariner 9 began systematic mapping of the Martian surface on January 2, 1972. Since that time, although original plans called for mapping of only 70 percent of the planet's surface, 85 percent of the surface of Mars has been mapped. About 7000 television pictures have been obtained since early November.

On January 6, some extraordinary pits and hollows, never before seen on Mars, were photographed by Mariner 9 from a range of 3343 kilometers (2072 miles; see Figure 21). Located about 800 kilometers (500 miles) from the Martian south pole, these features have raised some interesting questions regarding the geologic processes that have shaped the landforms of the polar region. These structures may have resulted from the thawing of large accu-

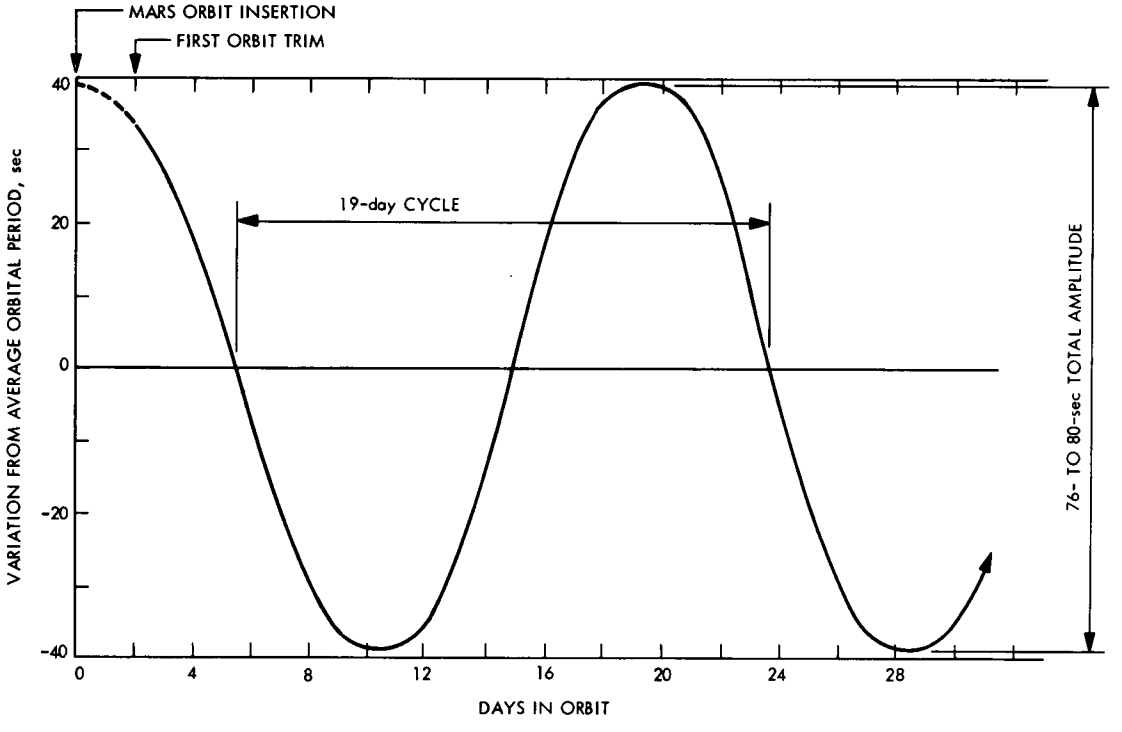

Figure 20. Effect of variations in the gravity field on the Mariner 9 orbital period.

Figure 21. Mariner 9 picture showing pits and hollows never before seen on Mars. The two large, closed basins at left are about 16 kilometers (10 miles) across. The small pits are 1-1/2 to 3 kilometers (1 to 2 miles) wide.

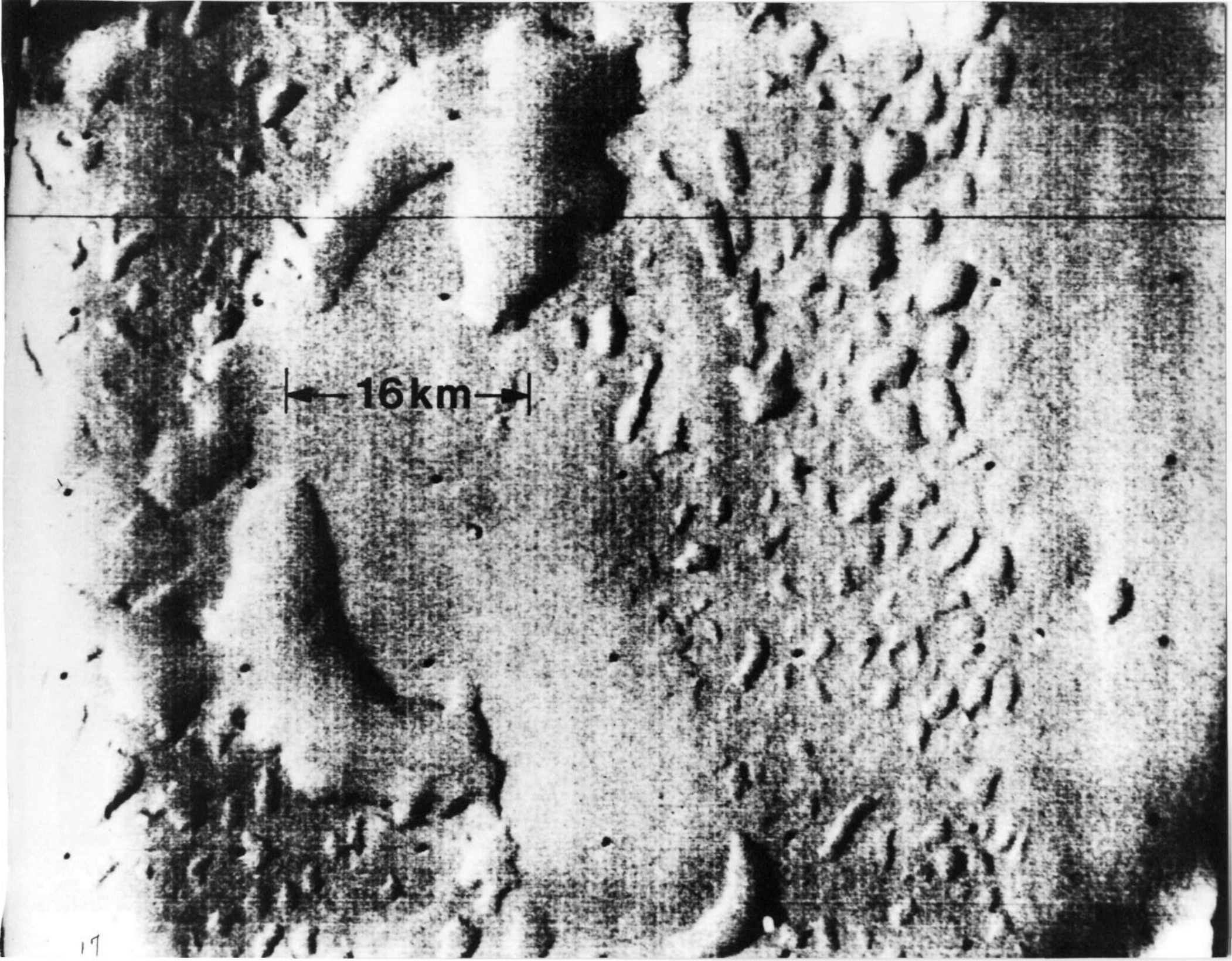
16km

mulations of ground ice or may be deflated hollows developed by wind action in loosely consolidated material. A complex pattern of delicate swirls and blotches, which cloak the south polar region, is shown in Figure 22. The area covered in the picture is about 80 by 100 kilometers (50 by 62 miles) and is located at about 80° south latitude.

The first clear view of rilles (cracks) in the Martian crust was obtained on January 7 in Mare Sirenum (see Figure 23). These structures are part of a system of parallel fissures extending more than 1800 kilometers (1100 miles) along the surface. Lunar rilles have been interpreted as tensional features produced by stretching of the upper rock layers. The same origin seems probable for the Martian rilles.

The Martian canyonlands, part of a 120,000-square-kilometer (46,300-square-mile) complex in Noctis Lacus on the northern edge of the Solis Lacus region, also were photographed by Mariner 9. The canyons, about 10 to 20 kilometers (6 to 12 miles) wide, have smooth floors and are separated from one another by flat-surfaced plateaus. The Martian canyons may be as deep as 6 kilometers (4 miles), and the walls slope 10 to 15 degrees. Their overall dimensions are similar to those of the Grand Canyon in Arizona. The linear segments of the canyon walls are roughly parallel to one another. Observations suggest that the canyons are of structural origin, but the intricate fluting of the walls indicates erosional modification. An intricate network of canyons is shown in Figure 24. The picture, which covers an area 542 kilometers wide by 426 kilometers high (336 by 264 miles), shows evidence of the erosion processes.

The clearer atmosphere revealed Nix Olympica as a mountain 500 kilometers (310 miles) wide at the base (see Figure 25). Steep cliffs drop off from the mountain flanks to a surrounding great plain. The main crater at the summit, a complex multiple volcanic vent, is 65 kilometers (40 miles) wide. The mountain is more than twice as broad as the most massive volcanic pile on Earth. The mountain that forms the Hawaiian Islands is 225 kilometers (140 miles) across and rises 9 kilometers (6 miles) from the floor of the Pacific to the summit crater, Mauna Loa.

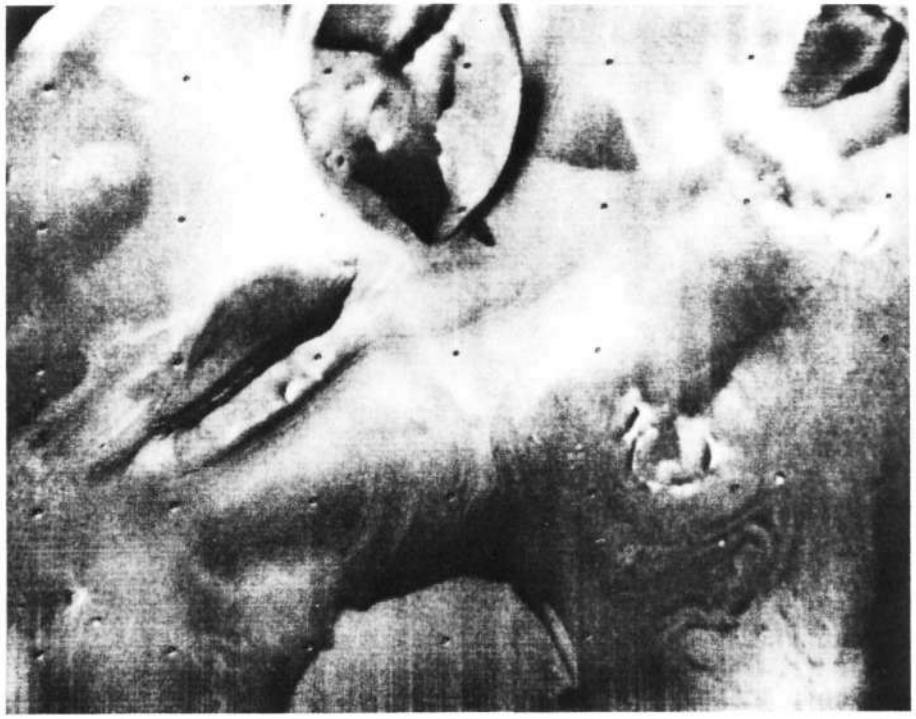

Figure 22. Picture showing complex pattern of swirls and blotches. Dark splotches at lower left, right center, and bottom center are on the floors of surface depressions.

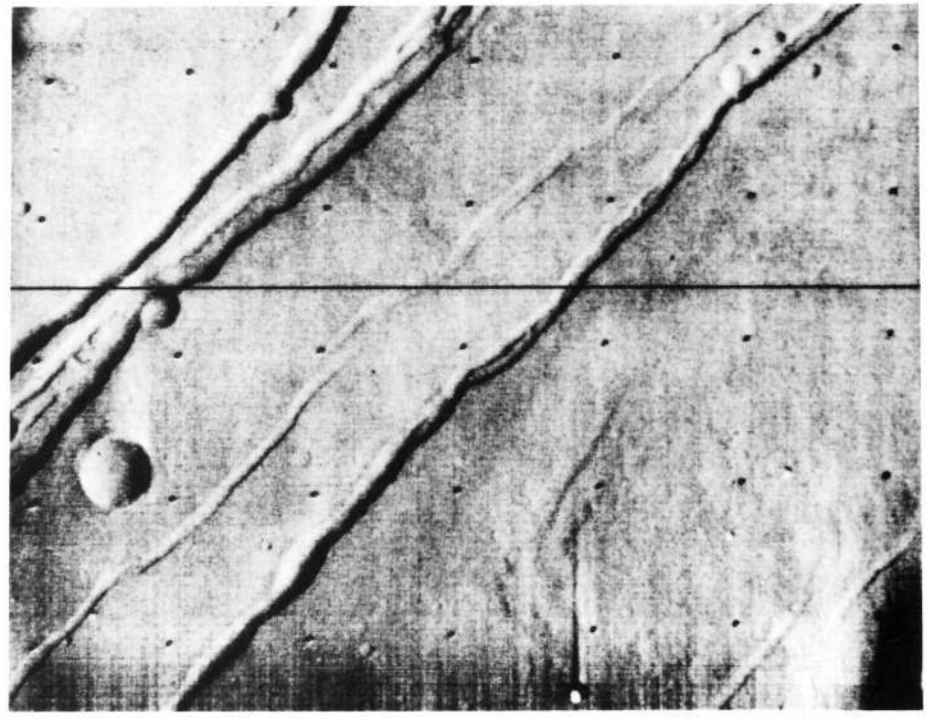

Figure 23. Rilles in the Martian crust. The widest rille, at upper left, is about 1-1/2 kilometers (1 mile) across and contains a more shallow rille in its floor. The diagonal rille across the center of the picture is about 40 kilometers (25 miles) long.

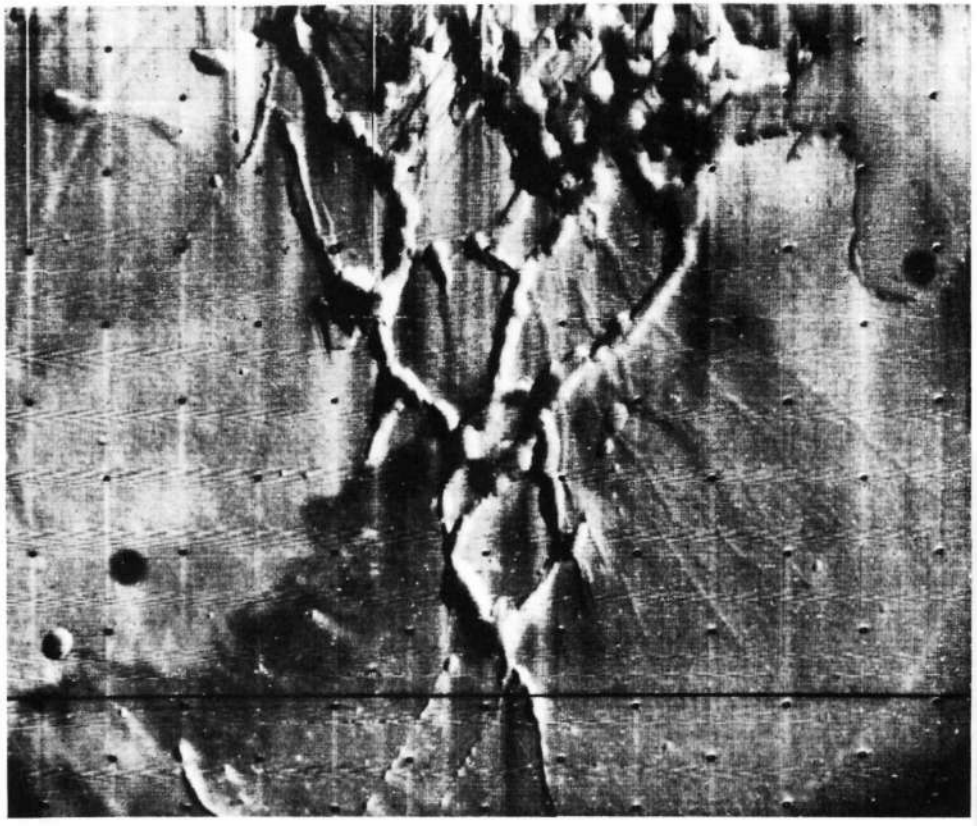

Figure 24. Network of Martian canyons.

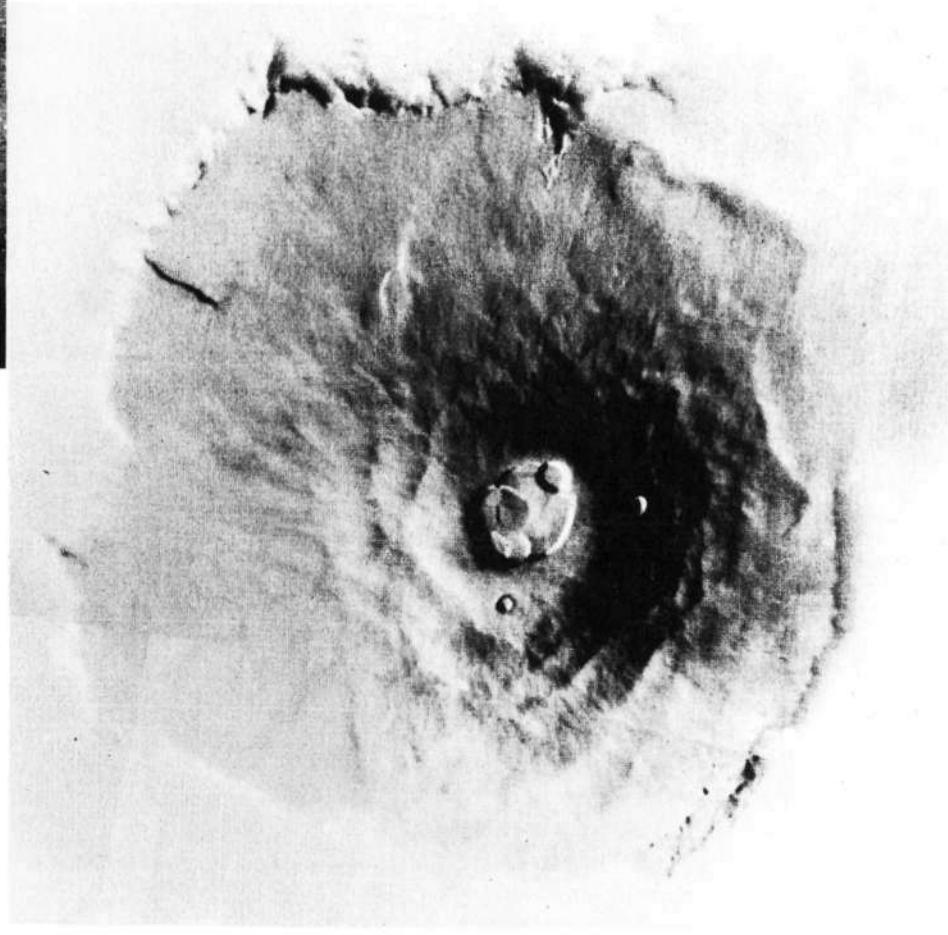

Figure 25. Computer-processed picture of Nix Olympica photographed by Mariner 9 in late January 1972.

Toward the end of the mapping mission, features of special interest were studied such as the braided channel sweeping past a crater 19 kilometers (12 miles) wide (see Figure 26). This channel suggests the former presence of fluid erosion of the Martian surface. However, the meandering "river" (see Figure 27), though not unique on the Martian surface, is the most convincing evidence that a fluid once flowed along the surface, draining an extended area and eroding a deep channel. Landforms are being studied in detail to determine whether water or some other fluid system was the active agent. Light and dark streaks, which usually originate at small topographic features such as craters and bumps, were observed over widely separated regions of the Martian surface (see Figure 28). Elongated patches of similar albedo are roughly parallel within a region, suggesting that their formation is related to erosion and/or deposition by Martian winds.

With the dust subsiding, the ultraviolet spectrometer was able to penetrate to the surface. Using the physical process called Rayleigh scattering, the topography of Mars was examined, providing a third dimension of information (height) to the television pictures. Comparison of pressure measurements made by the ultraviolet spectrometer with a mosaic of two pictures of the Tithonius Lacus region on Mars revealed a vast canyon four times as deep as Earth's Grand Canyon (see Figure 29). The Martian canyon is estimated from ultraviolet spectrometer data to be 6 kilometers (19,700 feet, or about 3-3/4 miles) deep and 120 kilometers (75 miles) wide. (Earth's Grand Canyon is 1.7 kilometers (5500 feet) deep and 21 kilometers (13 miles) wide. The vast chasms and branching canyons represent landform evolution apparently unique to Mars. Subsidence along lines of weakness in the crust and sculpturing by winds are believed to have formed the features.

Figure 26. Two-picture mosaic showing braided channel sweeping past a crater. Both pictures were taken from an average range of about 1800 kilometers (1116 miles).

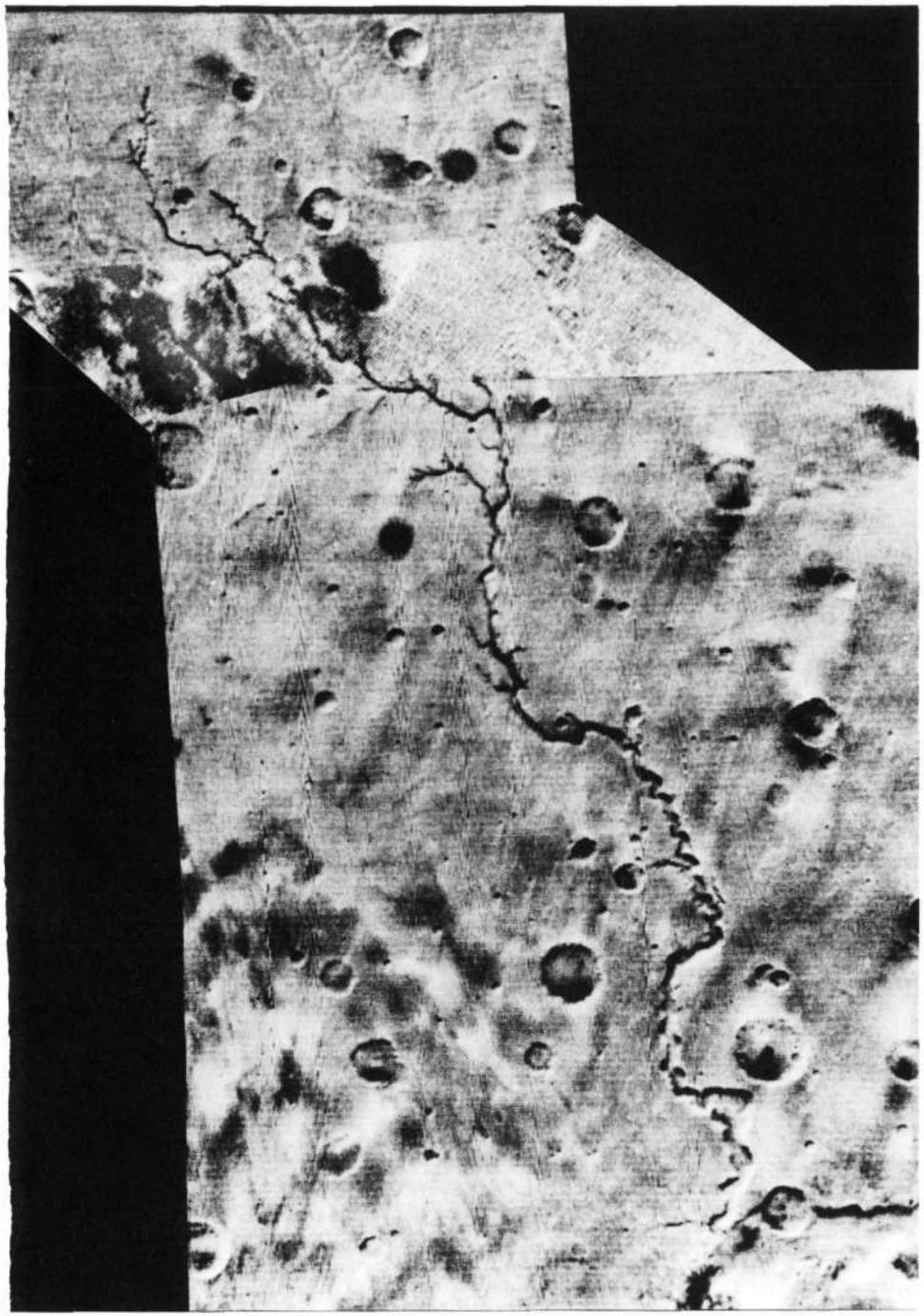

Figure 27. This meandering "river", about 575 kilometers (355 miles) long and 5 to 6 kilometers (3 to 3-1/2 miles) wide, resembles a giant version of an Earth "arroyo" . . . a watercut gully found frequently in the mountainous southwestern United States. The feature extends from 38° to 45° west longitude and 27° to 30° south latitude.

Figure 28. Light and dark streaks, each associated with a crater, appearing in the Juventas Fons region of Mars.

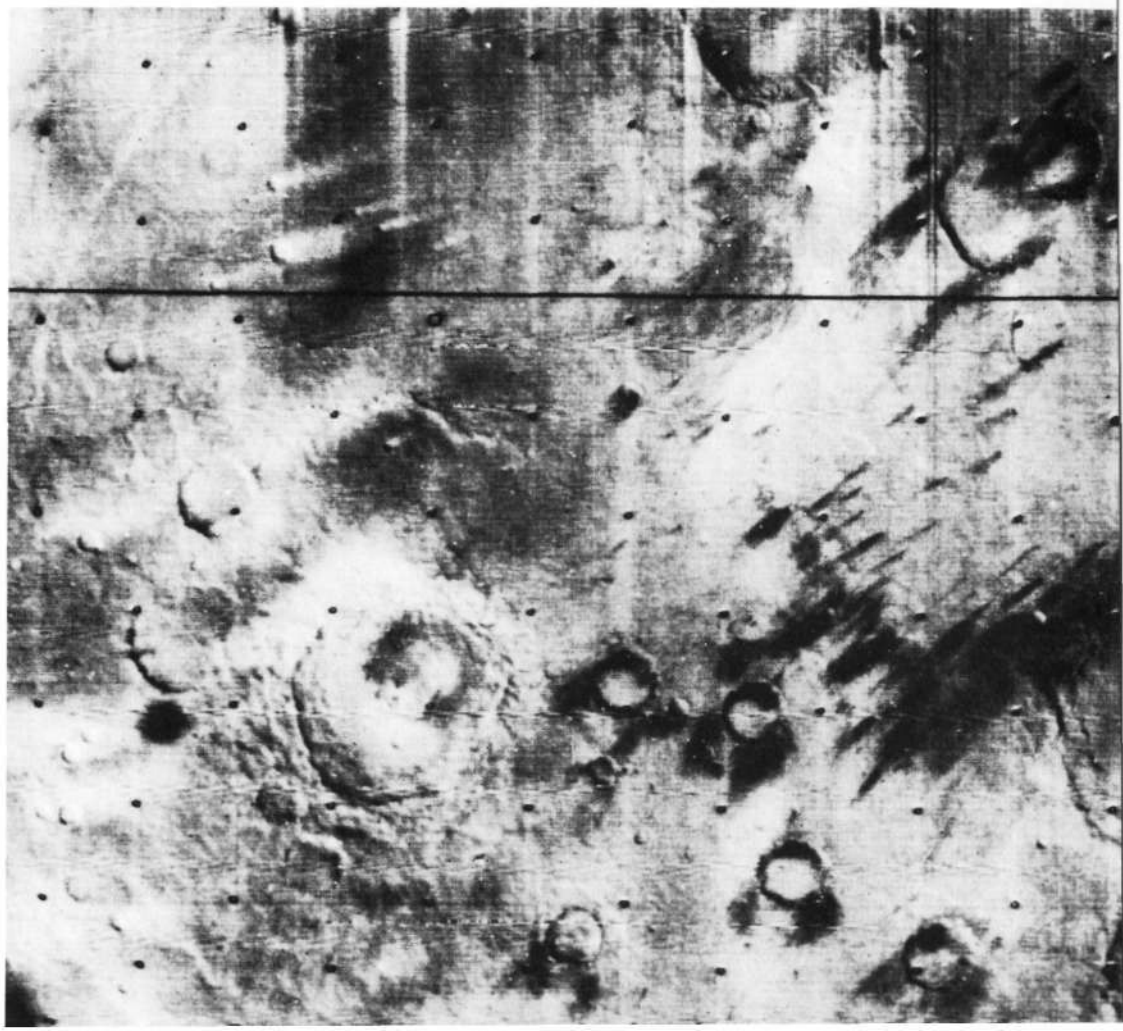

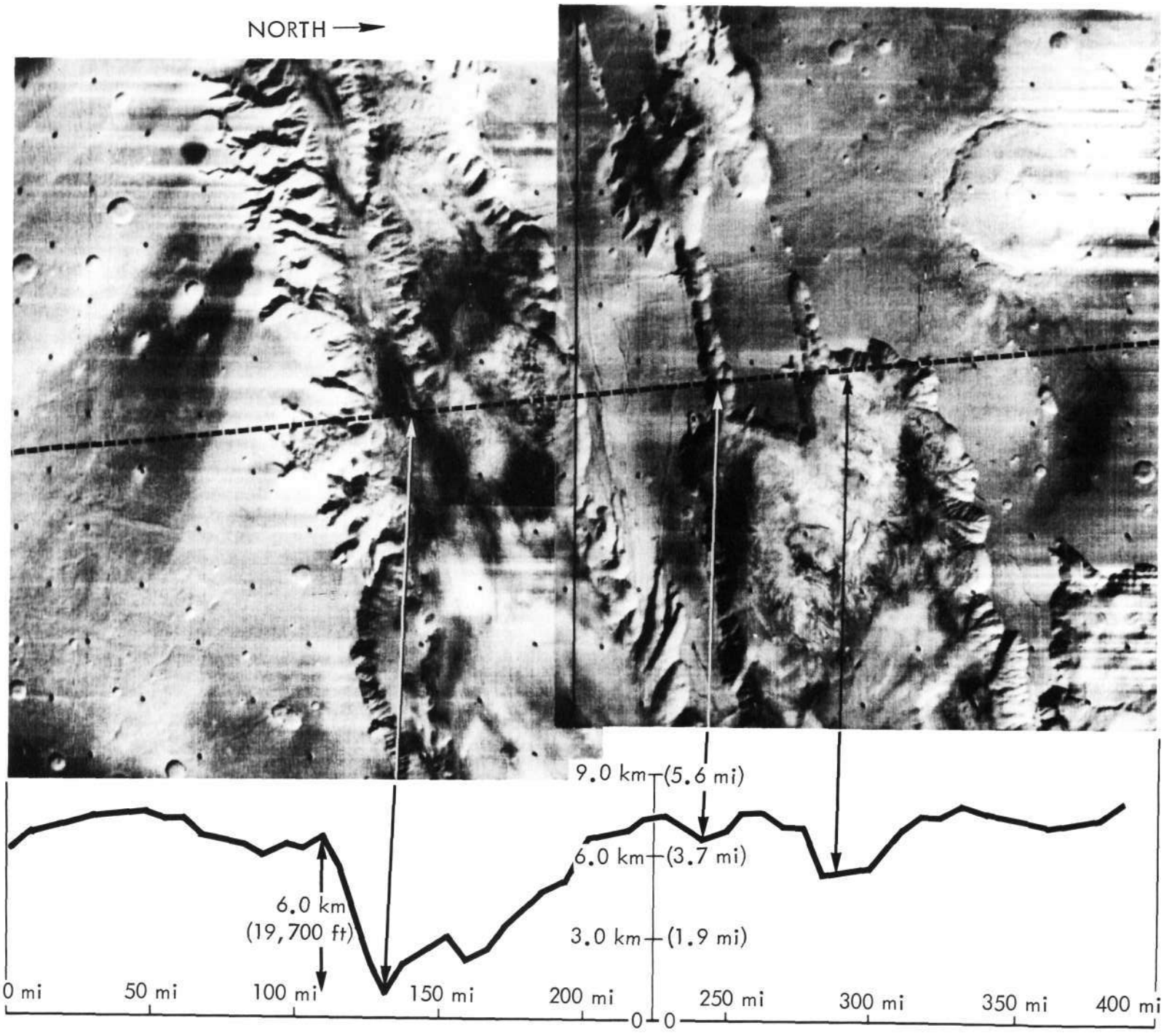

Figure 29. Two-picture mosaic of the Tithonius Lacus region, revealing a canyon four times as deep as the Grand Canyon in Arizona. The white arrow at left points to the Martian canyon. The jagged line at the bottom of the figure represents ultraviolet spectrometer pressure measurements, which are translated into heights. The dotted line through the picture is the instrument's scan path across the surface. The two arrows at right also relate low points to the ultraviolet spectrometer measurements.

Figure 30. Clouds of a type not uncommon on Earth on the lee side of mountains. The only surface detail visible here is a frost-rimmed crater about 90 kilometers (56 miles) wide. The flow of air over the crater rims produces wave clouds that propagate for several hundred kilometers.

Spectra from the ultraviolet spectrometer showed that the atmosphere is composed primarily of carbon dioxide with small amounts of carbon monoxide, oxygen, and a few other minor constituents that result from the photochemistry of a carbon dioxide atmosphere with a small amount of water.

Measurements performed in the upper atmosphere of Mars (above 100 kilometers) show the presence of atomic hydrogen, atomic oxygen, and carbon monoxide as the neutral species; the ionosphere contains ionized carbon dioxide, carbon monoxide, and ionized molecular oxygen. The amount of ionization is variable with location and time above the planet and may depend upon the Sun's radiation input to the upper atmosphere of Mars. The atomic hydrogen signal observed by the ultraviolet spectrometer also varies with time and location. Correlation of the Mars atomic hydrogen Lyman alpha signal (1216 angstroms) with observations of the influence of the Sun on the Earth's atmosphere shows that the atmosphere of Mars is responding primarily to solar photon radiation rather than the solar wind. This is

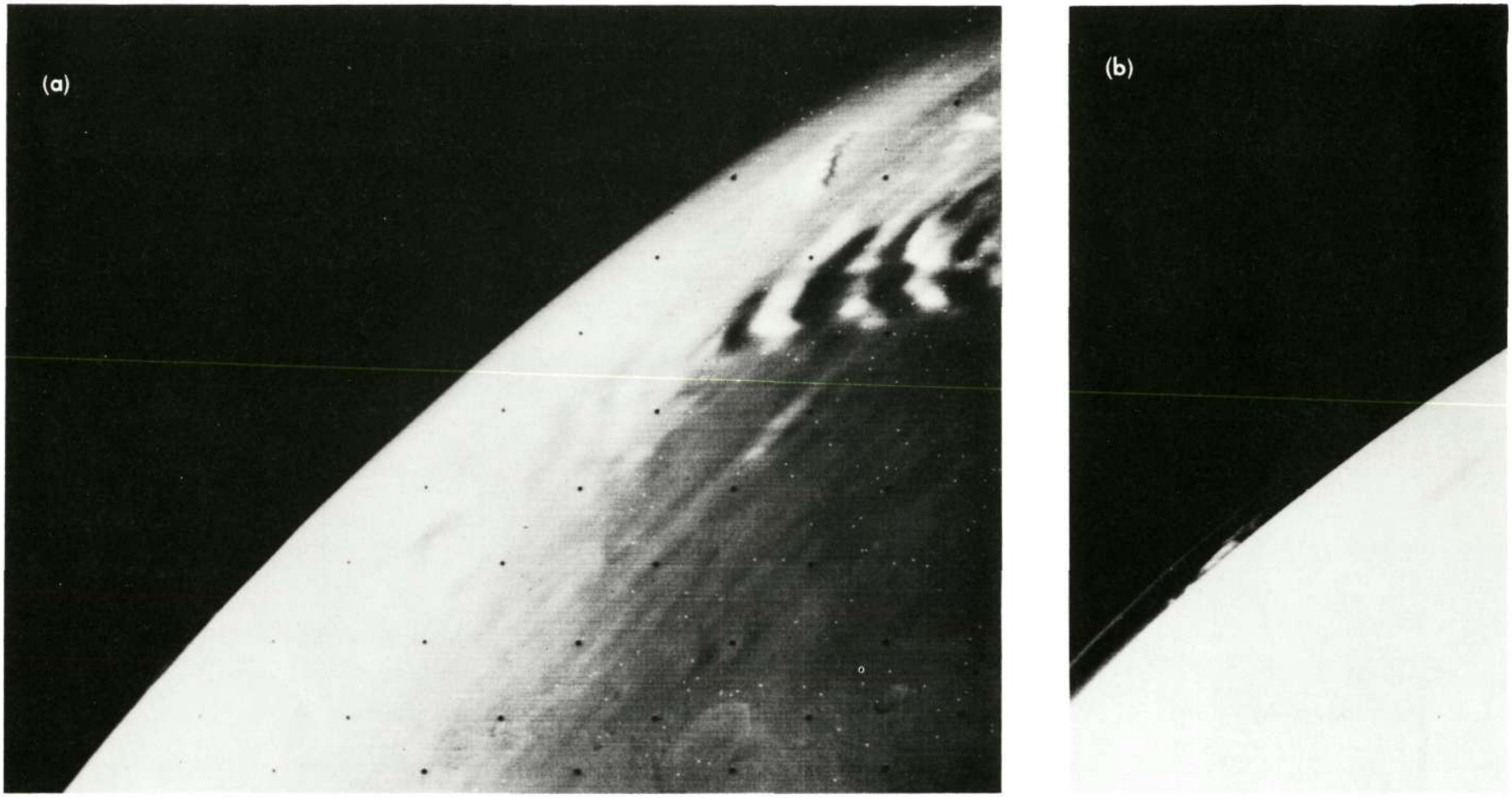

Figure 31. Thick wave clouds viewed by Mariner 9. (a) Wave formation in the twilight lighting. (b) The same feature observed the next day as a silhouette on the limb of the planet.

determined by observing the time lag between the response of Earth's atmosphere to the variable solar flux when compared with the Martian atmosphere.

The loss of atomic hydrogen from the planet also was measured by the ultraviolet spectrometer. If the source of the hydrogen were from water, the loss would be equivalent to 2-1/2 centimeters (1 inch) of rain over an area about 9-1/2 meters (30 feet) wide and about 1-1/2 kilometers (1 mile) long, or about 100,000 gallons of water per day. This is not as alarming as it seems; this quantity of water could have been lost from Mars each day since the planet was first created and still would represent less than 1 percent of its total available water.

One of the observations made by Mariner 7 in 1969 was that there appeared to be ozone on or above the south polar cap. However, no confirmation of the presence of ozone was observed by Mariner 9. After December 30, when observations of the north polar region were possible (above 40° north latitude), the absorption spectrum of ozone was observed everywhere in the north polar hood. During this same time period, observations of the south polar area continued to show no presence of ozone until the change of the Martian season. With the southern hemisphere entering the Martian fall in March 1972, the ultraviolet spectrometer observed an increase in reflected

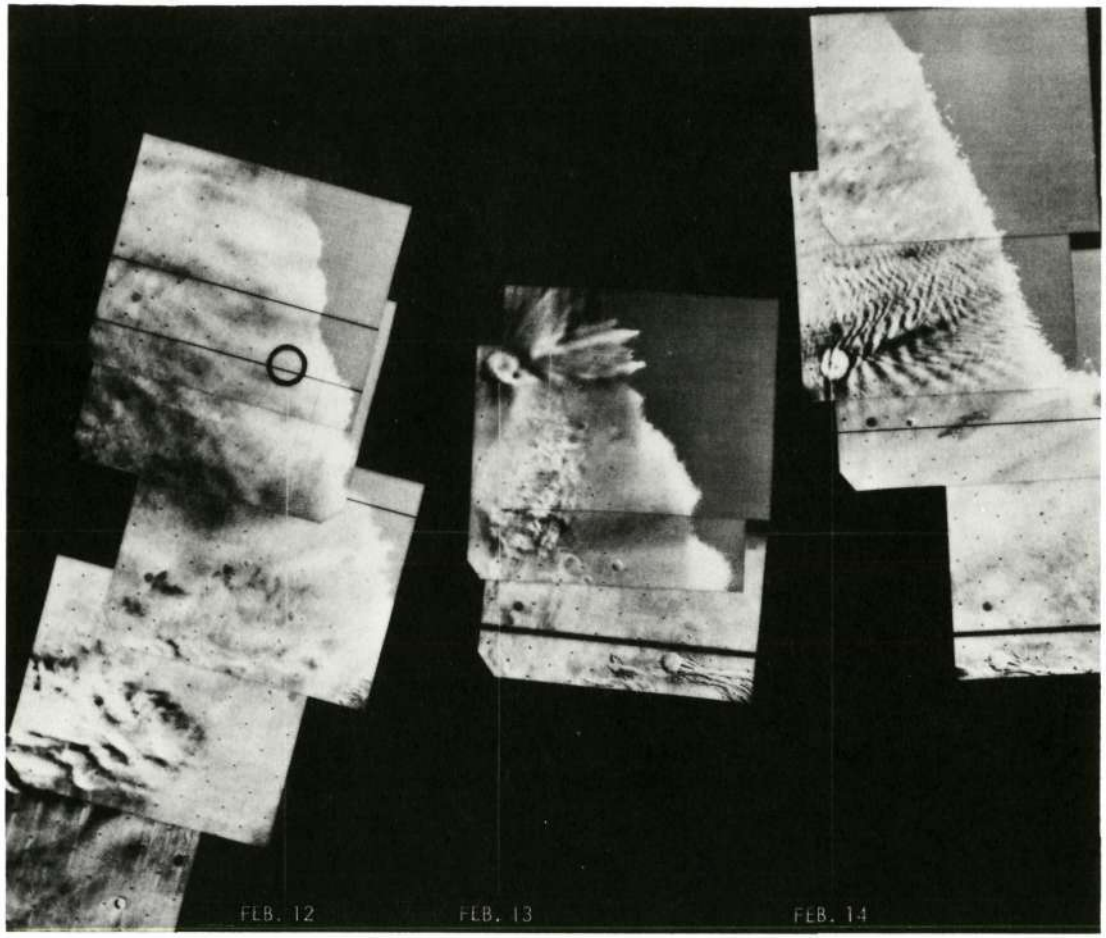

Figure 32. Atmospheric changes observed on 3 successive days. The circle in the February 12 picture indicates the location of the crater visible in the February 13 and 14 pictures and shows the apparent perturbations emphasized by the cloud pattern.

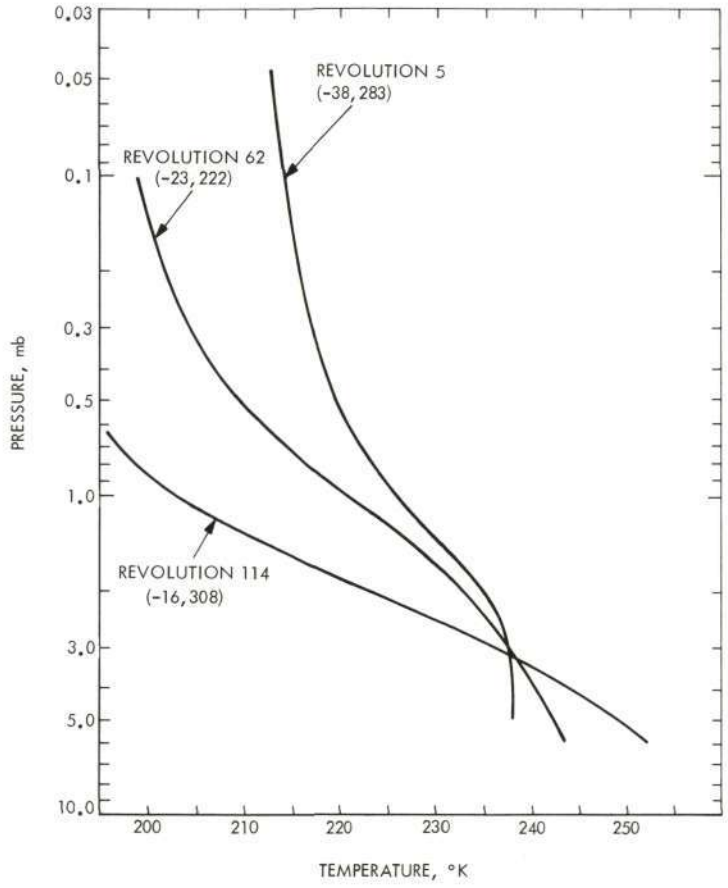

Figure 33. Representative Martian atmospheric temperature profiles, going from isothermal to almost adiabatic. Profiles were obtained from infrared interferometer spectrometer data on November 16, December 14, and January 9.

light near the south polar cap. This has been interpreted as the onset of a south polar haze. Associated with this haze was the presence of the ozone absorption spectrum. With the approach of winter in the southern hemisphere, the ozone concentration in the south has continued to increase.

An unanticipated "bonus" derived from the mission was the observation of young stars in the ultraviolet portion of the spectrum. Measurements of these stars cannot be made from Earth because the Earth's atmosphere absorbs the ultraviolet part of the spectrum. The observations will supply information about the evolution of these stars . . . whether or not they have gas clouds about them, and whether they are in regions of space in which large amounts of galactic dust exist.

Throughout the Mariner 9 mission, Mars has been experiencing winter in its northern hemisphere. During this season, latitudes above about 45° north have been blanketed by clouds such as shown in Figure 30. A patch of thick clouds observed at 54.8° north latitude is shown in Figure 31a; these same clouds were viewed the next day silhouetted on the limb of the planet (Figure 31b). Pictures of the same region showing atmospheric changes on successive days are shown in Figure 32. Data from the infrared instruments indicate that the cloud deck is consistent with that of condensed carbon dioxide.

As mentioned previously, the atmospheric temperature profiles obtained by the infrared interferometer spectrometer reflect the thermal coupling between the Sun, Mars, and the Martian atmosphere; as such, they are a sensitive indicator of the amount of obscuration by the dust in the atmosphere. A significant change in the lapse rate, from nearly isothermal to nearly adiabatic, was observed (see Figure 33) at about the same time that the television picture contrast improved.

Temperature profile swaths such as those of Figure 34 have provided valuable information about various aspects of Martian meteorology including thermal inversions, wind fields, and the formation of lee waves.

The 15-micrometer carbon dioxide band contains, in addition to information about atmospheric temperature profiles, information about the pressure of carbon dioxide at the surface. Variations of carbon dioxide pressure, related to altitude variations, by means of the barometric law, can provide topographic information. Topographic maps derived from surface pressure measurements by the infrared interferometer spectrometer are shown in Figures 35 and 36. The altitudes range from -3 to +14 kilometers (-2 to +9 miles) referenced to an assumed 6.1-millibar pressure level.

The lower atmosphere is composed primarily of carbon dioxide and small amounts of water vapor in the range of 10 to 20 precipitable micrometers, except in the north polar region where no water vapor was observed. (One precipitable micrometer is an amount of water vapor which, if condensed, would form a film of water one-millionth of a meter thick.) Ozone was observed only in the polar hoods. No other polyatomic constituents (e.g., molecules) and no significant variations in time or in space have been detected.

Weak reststrahlen features were observed, even after the clearing of the atmosphere. If it can be shown that these arise from the surface, the infrared interferometer spectrometer should eventually provide maps of the Martian surface in the silicon oxide range (i.e., rock and mineral types). Comparison of these data with visual

Figure 34. Isotherms for a cross section obtained in the north polar region on January 3, 1972. The boundary temperature at the bottom of the figure represents the interface between the surface and the atmosphere.

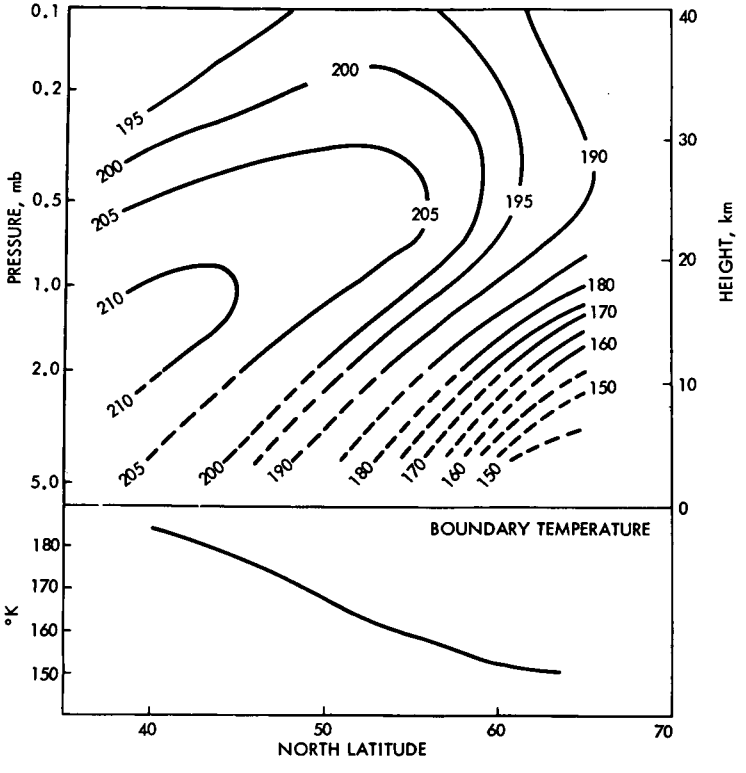

Figure 35. Topography of Hellas basin. The Hellas basin is the lowest known Martian feature, measured as 3 kilometers (10,000 feet) below the 6.1-millibar level. All contours shown are in kilometers.

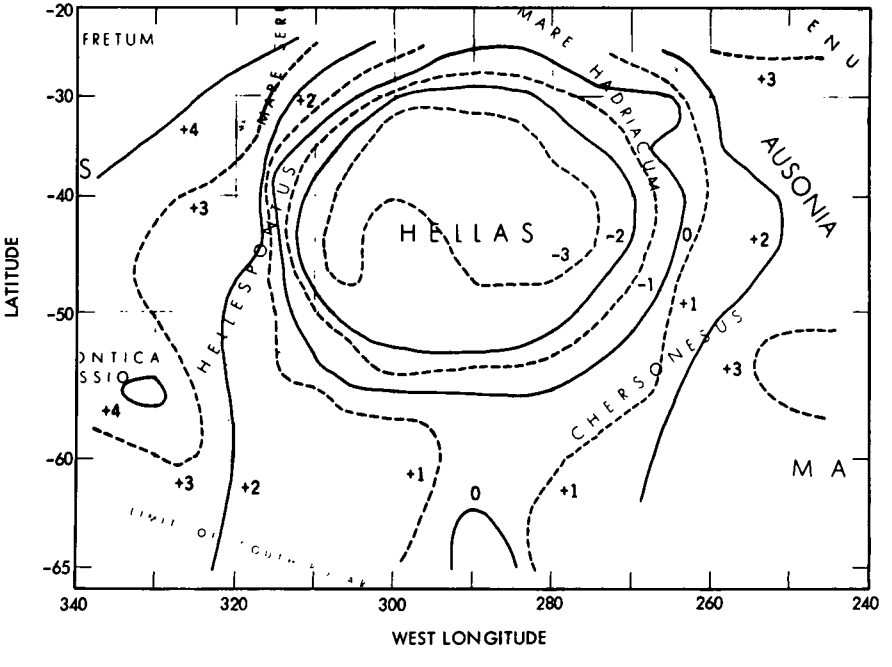

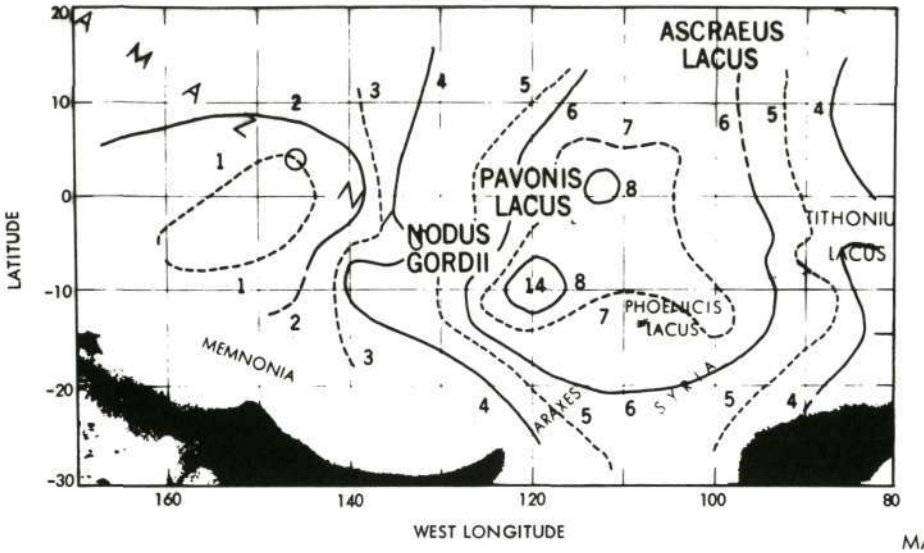

Figure 36. Topographic map of Tharsis region. The Amazonis–Tharsis region includes the Nodus Gordii volcano, which rises 14 kilometers (9 miles) above the 6.1-millibar level. All contours shown are in kilometers.

observations will help to increase our understanding of Martian geology.

The infrared interferometer spectrometer has provided information that negates the recent concept of Mars as a "dead planet". The atmosphere is active and the planet has been differentiated.

After the dust cleared and the surface could be seen, the infrared radiometer data showed that the temperatures correlate more closely with those predicted from 1969 data. There are some deviations due to albedo and some differences in thermal characteristics. Some areas do not cool at night as much as predicted and are about 195°K (-109°F) instead of 180°K (-136°F). The surface is proving to be nonhomogeneous. South Spot, as viewed by the infrared radiometer, is shown in Figure 37.

Because the celestial mechanics and S-band occultation experiments use radio tracking signals to acquire data rather than a specific instrument, their activities were not hampered

Figure 37. Infrared radiometer's view of South Spot. The line through the picture of South Spot indicates the instrument's view. The plot above shows the temperature measurements obtained from the data; relative altitude can be inferred from the temperature and the Sun angle.

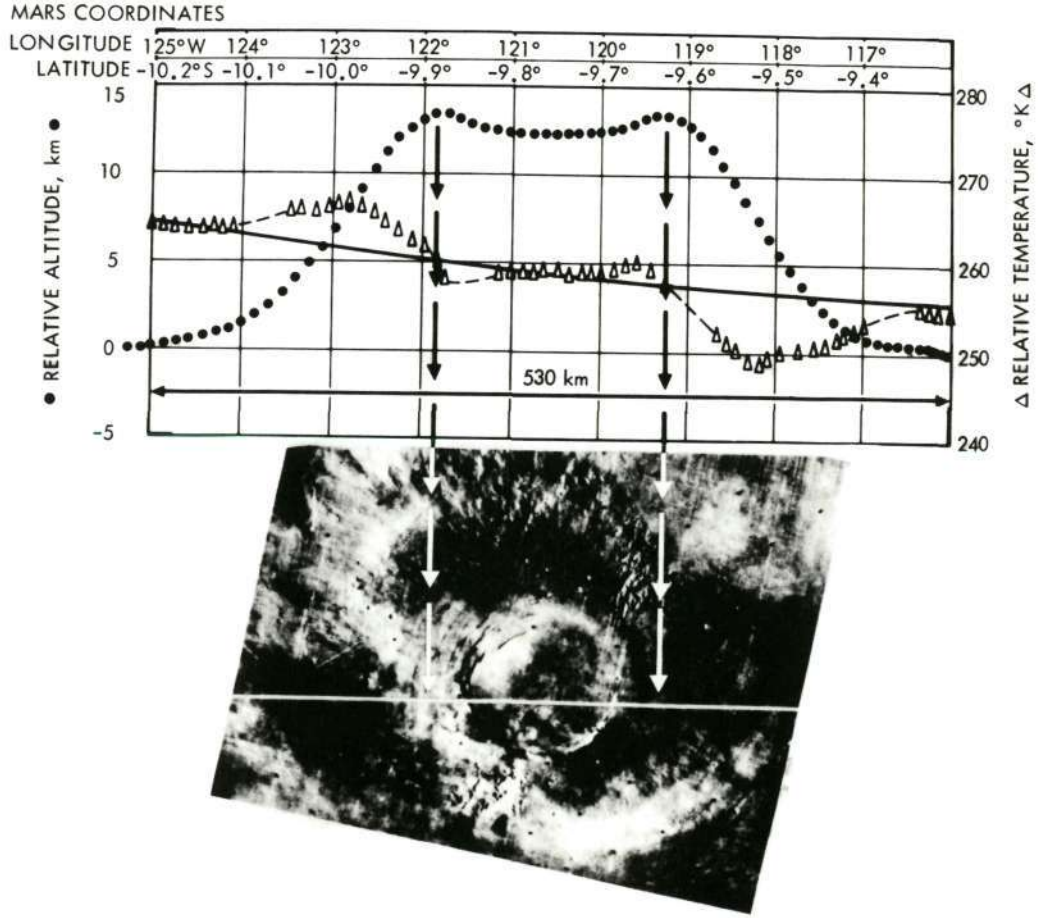

by the atmospheric dust. Values for some of the basic constants for Mars such as mass, oblateness, and orientation of the pole were confirmed and improved by the celestial mechanics experiment. However, their primary findings apply to the gravity field.

If Mars were a spherical, smooth shape, and if it were composed of uniform-density material (or even various-density material that had the same density as other material at the same distance from the center of the sphere), the gravitational pull of Mars would be uniform. For various reasons, no bodies in our solar system have smooth or uniform gravity fields.

A gravity map of part of Mars is shown in Figure 38. The northern hemisphere is omitted because the spacecraft passed in back of Mars and thus could not be observed when it was over the northern hemisphere during the early part of the mission. Figure 39 shows the Mariner 9 gravity profile compared with the actual surface topography measured by Earth-based radar along a section at about 15° south latitude. The Mariner 9 profile is from data obtained between November 16 and December 4, 1971. Radar is from Goldstone and Haystack data obtained during the summer of 1971. The two profiles agree well, suggesting that the geologic mechanisms leading to relief of gravitational stresses are not dominant on Mars.

Because Mariner's orbital path no longer carried the spacecraft in back of the planet, as

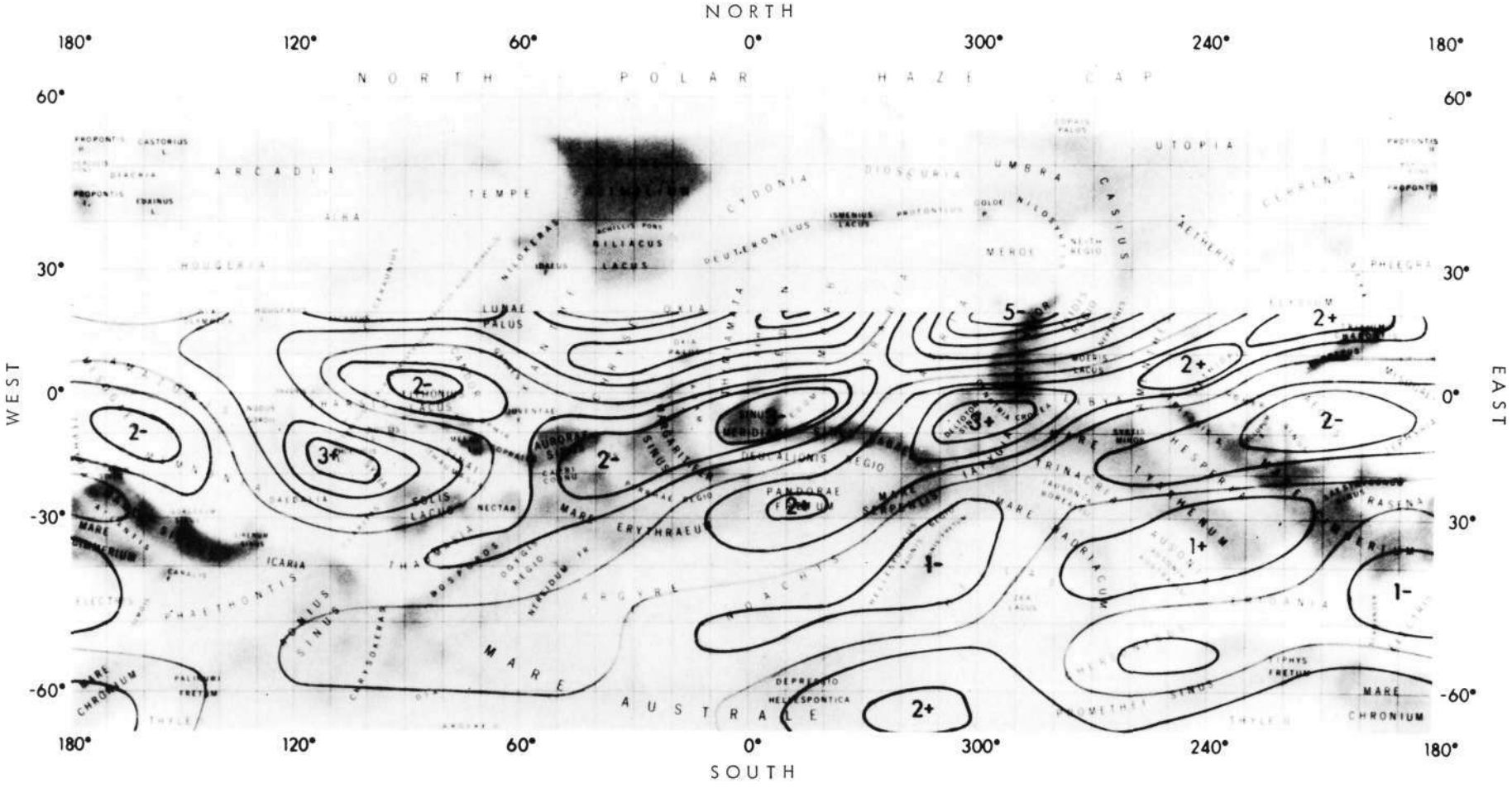

viewed from Earth, there were no S-band occultations from the end of December 1971 to the beginning of May 1972. However, more than 150 entry and exit occultation points were measured during the 90-day standard mission (see Figure 40). May and June provided a second set of occultation data; a third set of occultation points will start in September 1972.

The surface pressures in the near-equatorial and middle-latitude regions range from a high of 8.9 millibars in Hellas to a low of 2.8 millibars in the Claritas and Tharsis areas, with an average pressure of 4.95 millibars. The pressures derived from measurements at 65° north latitude range from 7.2 to 10.3 millibars, with an average of 8.9 millibars.

Pressure altitudes derived from the S-band occultation experiment, referred to a pressure level of 6.1 millibars, range in the equatorial regions from a low of -4.4 kilometers (-14,436 feet) in Hellas to a high of 9.6 kilometers (31,500 feet) in Claritas, with a

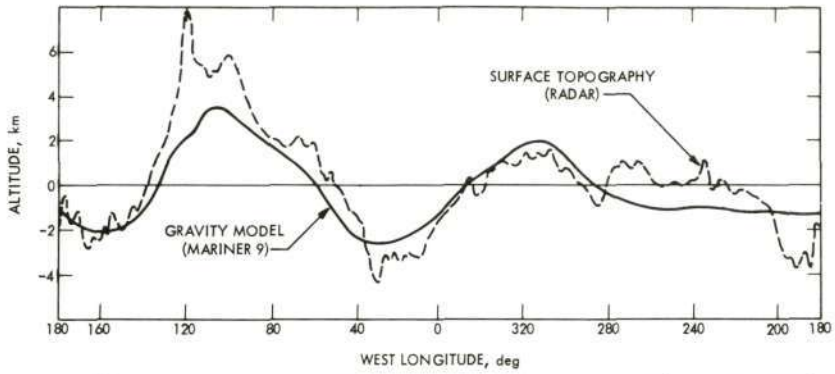

Figure 40. Mariner 9 gravity profile compared with the surface topography measured by Earth-based radar at 15° south latitude.

Figure 39. Locations on Martian surface of entry and exit occultation points. Revolution numbers are indicated next to locations; those above revolution 79 are a second-set of occultation points that occurred in May and June of 1972.

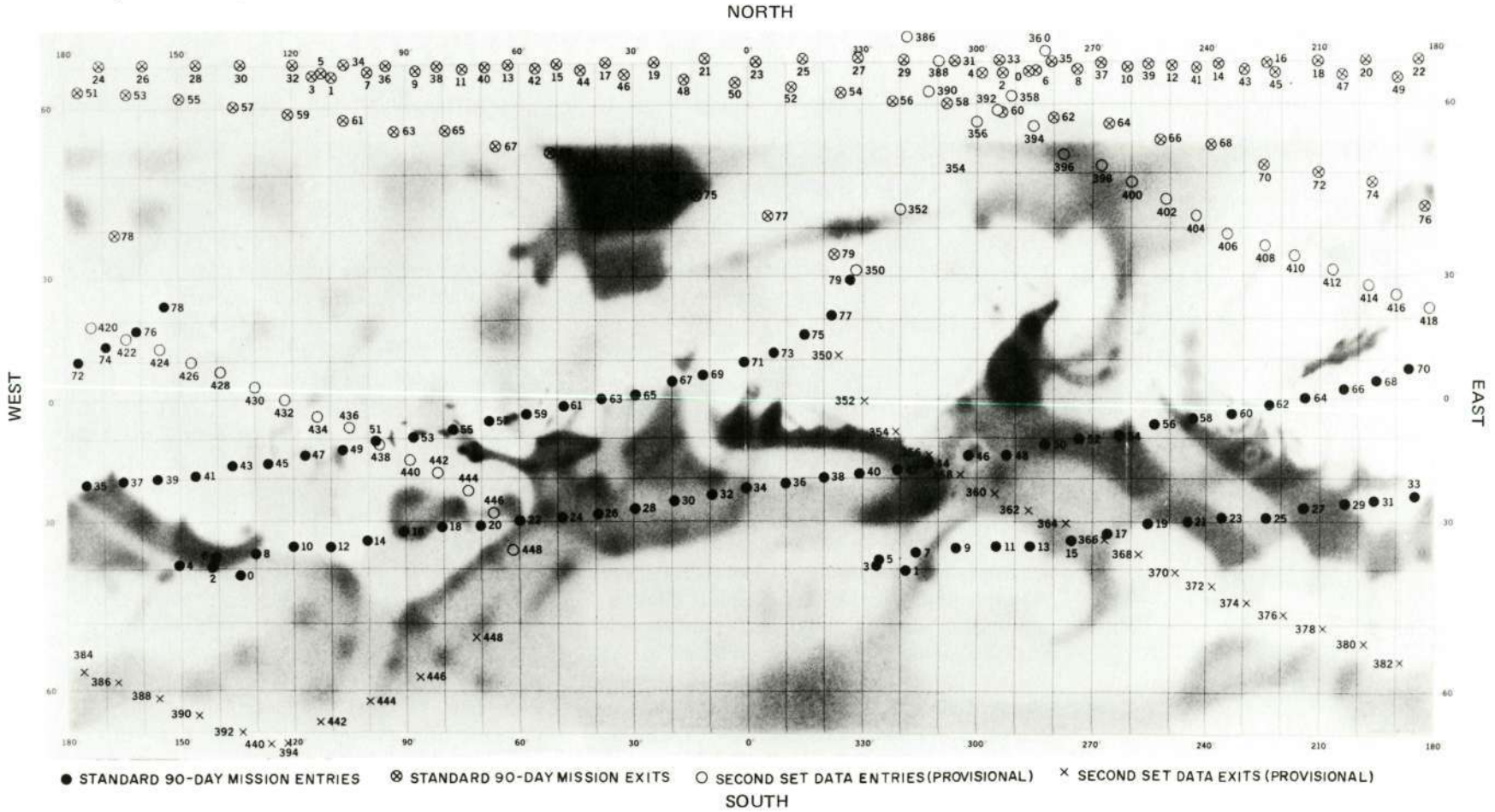

net excursion of 14.0 kilometers (45,900 feet) and an average altitude of 2.7 kilometers (8900 feet). In contrast, the region at 65° north latitude shows uniformly negative altitudes, with an average of -2.6 kilometers (-8500 feet). This disparity in pressures, which is also reflected in the measured radii, between the near-equatorial and 65° north latitude measurements, strongly suggests that the physical shape of Mars is more oblate than the shape of a gravitational equipotential surface.

A daytime ionosphere with a peak density of about 1.5 to 1.7 X 10^5 electrons/cm^3 at an altitude of 140 to 134 kilometers (88 to 84 miles) was measured over a range of solar zenith angles of 56 to 47 degrees (Figure 41), and shows some correlation between the variations in the peak density and terrestrially measured solar flux. The average topside plasma scale height was 38-1/2 kilometers (24 miles), showing little correlation with solar flux and solar zenith angle.

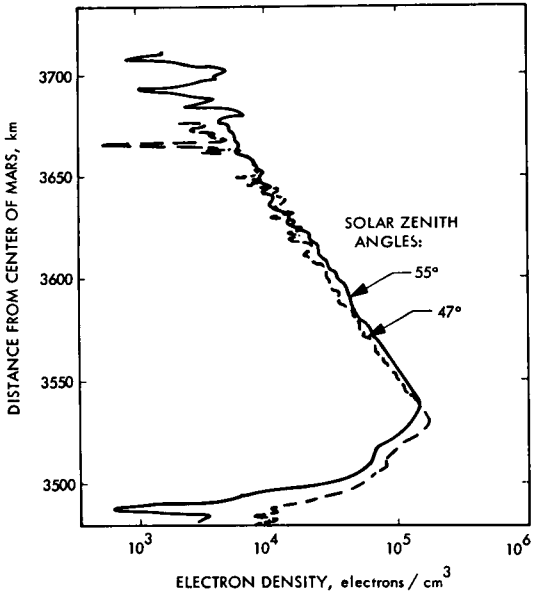

Figure 41. Typical electron density profiles derived from S-band occultation data.

From April 2 through June 4, the Mariner 9 flight path took the spacecraft into the shadow of Mars briefly during each orbit, undergoing solar occultation. This reduced the amount of electrical power provided by the solar panels, requiring shutdown of the on-board science instruments for the entire period. Only the S-band occultation and celestial mechanics experiments were able to acquire data. On June 5, the science instruments once again were activated; on June 8, data were again recorded for relay back to Earth on June 9. Early results indicate that the obscuring north polar hood has diminished sufficiently for the television cameras to photograph the north polar terrain.

On September 7, superior conjunction with Mars will occur. (Earth and Mars will be on opposite sides of the Sun.) Mars, as viewed from Mariner 9, then will be within about 1 degree of the Sun, and the solar gravitational field will affect the radio transmission signals. Data recorded 3 weeks on either side of superior conjunction will help to verify Einstein's general theory of relativity (Figure 42).

Mariner 9, in its journey thus far, has recorded winds that exceed 200 kilometers per hour (120 miles per hour), and has observed both planet-wide and local dust storms. The National Aeronautics and Space Agency has stated that knowing the dynamics of a planetary atmosphere other than that of Earth is extremely valuable for the understanding of our atmospheric circulation (a problem of great significance to meteorologists) and for understanding the potential effects of pollution in the Earth's atmosphere. For example, Mariner 9 has observed the effects of the atmospheric dust on decreasing the surface temperature . . . valuable data for scientists trying to predict the level of smoke and smog that could trigger another ice age on Earth.

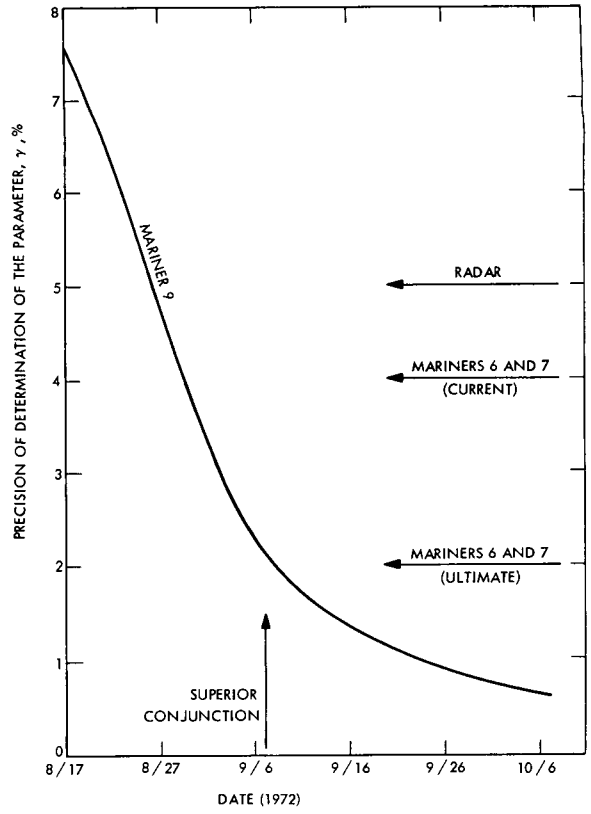

Figure 42. Improved test of general relativity to be made by Mariner 9.

Changes in surface features and varied atmospheric activity have been observed and recorded. Volcanoes and evidence of water ice have been observed. Although the volcanic processes of Mars are similar to those of Earth, they are in a better state for observation because erosion on Earth has obliterated much of its historical evidence. Thus, Mariner 9 data will help to improve our understanding of Earth . . . its history and its destiny.

All science instruments have performed successfully and all science objectives have been fulfilled. Considering that, of each federal tax dollar (for Fiscal Year 1972), 48 cents was spent on social concerns, 44 cents on defense, and only 1-1/2 cents on the entire space program, the information gained from the Mariner 9 mission, which will help to provide the answers to so many questions plaguing us on Earth, is a great bargain indeed.

To illustrate the impressive size of the canyonlands of Mars, they are shown here with an outline of the continental United States. The photomosaic was made from Mariner 9 pictures obtained over several weeks of photographic mapping of the surface. The area covered is located between 30° south latitude and 18° to 140° west longitude.

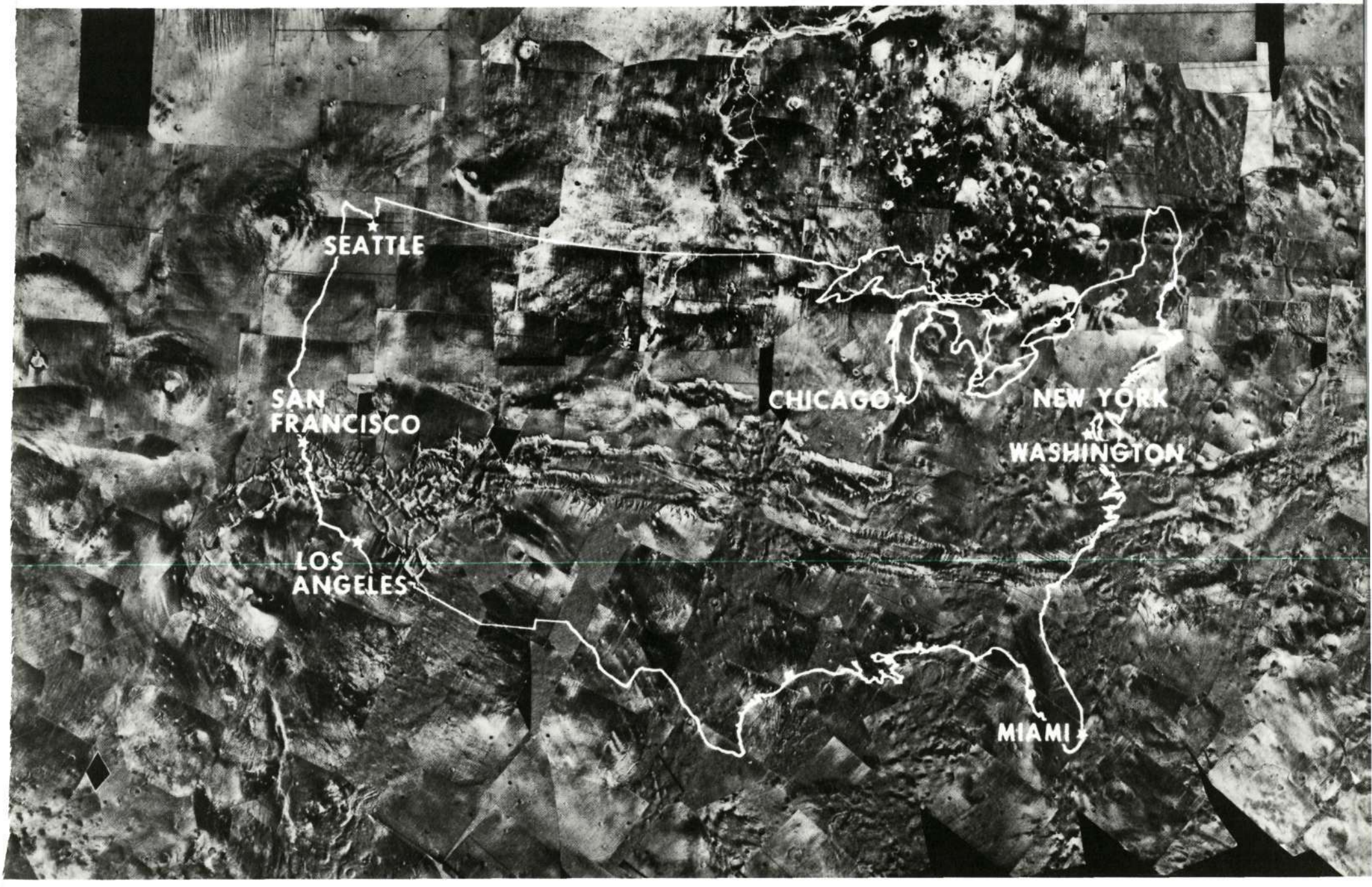

The success of Mariner 9 and the vast scientific results derived from the mission are due to the efforts of many persons. Especially recognized are the significant contributions of the following individuals:

NASA OFFICE OF SPACE SCIENCE: E. W. Glahn, Program Manager; H. Hipsher, Program Scientist; K. Wadlin, Program Engineer.

LEWIS RESEARCH CENTER: D. J. Shramo, Launch Vehicle System Manager.

JPL PROJECT STAFF: D. Schneiderman, Project Manager; J. F. McGee, Assistant Project Manager, Near Earth; E. Pounder, Assistant Project Manager, Near Planet; R. G. Forney, Spacecraft System Manager; R. Laeser, DSN Project Manager; P. J. Rygh, Mission Operations System Manager; N. R. Haynes, Mission Analysis and Engineering Manager, B.C. Houser, Project Control and Administration Manager; R. H. Steinbacher, Project Scientist; A. B. Whitehead, Assistant Project Scientist; T. Vrebalovich, Assistant Project Scientist.

PRINCIPAL INVESTIGATORS: C. A. Barth, University of Colorado, Ultraviolet Spectroscopy Experiment; G. A. Briggs, JPL, Television Experiment; G. de Vaucouleurs, University of Texas, Television Experiment; R. A. Hanel, Goddard Space Flight Center, Infrared Spectroscopy Experiment; A. J. Kliore, JPL, S-Band Occultation Experiment; J. Lederberg, Stanford University, Television Experiment; J. Lorell, JPL, Celestial Mechanics Experiment; H. Masursky, U. S. Geological Survey, Television Experiment; G. Neugebauer, California Institute of Technology, Infrared Radiometry Experiment; I.I. Shapiro, Massachusetts Institute of Technology, Celestial Mechanics Experiment; B. A. Smith, New Mexico State University, Television Experiment.

National Aeronautics and Space Administration
Jet Propulsion Laboratory/California Institute of Technology

Mariner Mars 1971 Project Office

JPL Technical Memorandum 33-559

June 1972